

Vicki Moon & Willem de Lange
School of Science
University of Waikato

1. Introduction

Following the exposure of a fault within a cutting in a new sub-division development in NE Hamilton, an initial investigation suggested the presence of 4 fault zones within the Hamilton Basin (Figure 1) that represented a potential hazard to infrastructure within the Basin. Hence, the overall aim of the proposal put to EQC was to *refine the locations of four potentially active faults within the Hamilton Basin*. To achieve this aim, two main phases of geophysical surveying were planned:

1. A seismic reflection survey along the Waikato River channel; and
2. Resistivity surveying to examine the sub-surface structure of identified fault zones.

Additional MSc student projects, funded by Waikato Regional Council, were proposed to map the surface geology and geomorphology, and assess the liquefaction potential within the Hamilton Basin.

During the course of the project, the initial earthworks for the Hamilton Section of the Waikato Expressway provided exposures of faults, which resulted in some modification of the project.

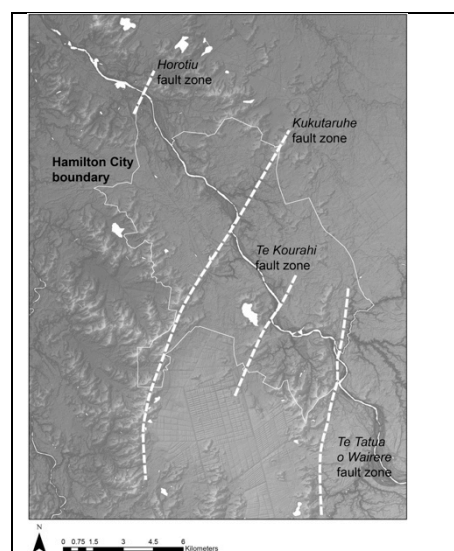


Figure 1: Map of the four fault zones that were initially identified from geomorphology and surface fault exposures, as presented in the original proposal.

2. Methods

The two main methodological approaches planned for this project were:

1. A high resolution CHIRP seismic reflection survey along the Waikato River within the Hamilton Basin. A previous study examining the stability of the river banks in response to fluctuating water levels (Wood, 2006) had obtained detailed data on the morphology of the river bed using multi-beam and single-beam echo sounders (MBES and SBES respectively), and side scan sonar. These data had shown the presence of unusual “scour holes” associated with zones of resistant material within the riverbed, some of which correlated with the fault zones shown in Figure 1. A seismic survey was proposed to determine if the scour holes were associated with faulting. Further, since the Waikato River is incised within the Hinuera Surface, it was suggested that any faults encountered would be less affected by the near surface splaying evident in the exposed fault in NE Hamilton, which would make them easier to detect.
2. Resistivity surveys would be undertaken along the trend of potential fault zones to confirm that faulting was present. This approach assumes that faulting will disrupt the groundwater systems within the fault zone, producing an identifiable pattern in the survey data. Initially 2D surveys were planned, but shortly after the project began the equipment and software were upgraded to allow the collection of 3D survey data. Subsequently 3D data were obtained. Geotechnical data, including boreholes, test pits, and CPT obtained for the development of an inland port close to the University of Waikato became available. This included an area identified as a potential fault zone, and allowed the results from various techniques to be compared.

However, in order to interpret the seismic data, and select suitable sites for resistivity surveys, a range of additional approaches were incorporated into the project:

1. Published and grey literature was searched for any existing evidence for faulting within the Hamilton Basin. This included a Summer Scholarship student who examined historical archives and oral traditions for accounts of earthquake impacts within the Waikato, focussing on the Hamilton Basin. The most useful information came from reports associated with the preparation of the 1:63,360 scale geological map, the coal resource surveys of the Waikato region, and seismic and borehole data obtained during oil and gas surveys of the Hamilton Basin. These reports identified faults around the periphery of the Hamilton Basin, which were inferred to continue into the Basin, and suggested the presence of a small volcanic field within the Basin (near Koromatua). In the absence of good evidence, these faults and volcanoes were not included in the more recent QMap series of geological maps.
2. High resolution LiDAR data provided by the Waikato Regional Council provided critically important evidence for surface morphologies associated with fault zones. Due to the small relief of the features, and the large amount of landscape modification by agriculture and urban development, they are difficult to spot in the field or from aerial photographs. However, within GIS it is possible to highlight the small gradient changes associated with fault zones, even within areas covered in peat that presumably smooths out any displacements over time. Using the locations of fault zones determined by seismic data, outcrops, or other evidence, LiDAR was used to trace the fault zones across the Hinuera Surface and predict where excavations or resistivity surveys would encounter fault zones. The earthworks associated with the Hamilton Section of the Waikato Expressway cut across the general trend of the fault zones in Figure 1, and so provide an opportunity to ground truth the fault zones mapped from LiDAR.
3. It was originally planned to undertake multiple seismic reflection surveys in order to assess the combination of frequencies and data acquisition settings that would allow fault zones to be identified. However, the data acquired during the first survey proved to be sufficient. Meanwhile, it was found that many of the potential fault zones occurred in areas where access to outcrops along the River was hazardous or difficult to obtain. Therefore, geological mapping and sampling along the banks of the Waikato River was undertaken by boat. Ground-based mapping and sampling in key areas that were accessible from the Hinuera Surface above the River supplemented this.
4. The excavation of deep cuttings along the northern half of the Hamilton Section of the Waikato Expressway provided exposures of faults through the hills within the Basin. To manage the environmental impact of the Expressway construction, the exposed faces are rapidly stabilised and covered. Therefore, it was decided that the MSc project that was intended to establish a site for trenching, would instead focus on documenting the faults exposed in cuttings while access was available.

The specific methodologies associated with the approaches summarised above is included in the following sections that focus on the results obtained with each approach. It is important to note that in general, the identification of fault zones within the Hamilton Basin is a consequence of multiple lines of evidence, which we consider contributes to a higher level of confidence in the interpretations.

Finally, while not specifically part of this project, the initial findings led to a re-examination of core data from peat lakes within the Hamilton and Hauraki Basins. This work has suggested that structures associated with tephra within the lakebed sediments represent seismites, and not bioturbation as previously assessed. Since the ages of the tephra layers are well constrained, these seismites may provide a useful measure of the frequency of strong seismic shaking within the Hamilton Basin. Further, if the conditions leading to the formation of seismites can be elucidated, then it would be possible to identify the minimum shaking intensity at each lake, and therefore provide an estimate of the earthquake location and magnitude.

3. Existing Literature

Previous reports on the geology of the Waikato region associated with the preparation of the 1:63,360 geological maps (N56 Ngaruawahia and N65 Hamilton) produced in the 1960s, an oil and gas survey in the 1970s, and a coal resource survey in the 1980s were examined. The findings were compared to the assessments produced as part of the Carbon Capture and

Storage (CCS) project by GNS in the 2000s. The key information from the existing literature is included here for reference.

3.1 Previously mapped faults

The Junction Magnetic Anomaly (JMA) lies along the western margin of the Hamilton Basin, and is considered to equate with the “Waipa Fault” (Figure 2). The Waipa Fault was originally mapped along the length of the Hamilton Basin with uplift to the west defining the boundary of the basin (Kear, 1960), despite the fault itself having no clear surface expression. It subsequently became evident during investigations into the coal resources of the Waikato that the character of the Waipa Fault differed north and south of the basaltic-andesite volcano, Mt Pirongia, which lies across the JMA near the centre of the Hamilton Basin (Kirk, 1991).

Through the section from Mt Pirongia north to the Hakarimata Range, the Waipa Fault is coincident with the JMA and displays considerable dip-slip movement (unlike other portions of the JMA in the North Island, which are dominated by strike-slip). Originally, Kear (1960) suggested that the Waipa Fault swung north-eastwards along the southern margin of the Hakarimata Range, before forming the eastern boundary of the Lower Waikato Basin (ultimately connecting to the Drury Fault to the north).

To the west of the JMA are typically Murihiku Terrane rocks; while to the east are typically Waipapa Terrane rocks. The Hakarimata-Taupiri Ranges at the northern margin of the Hamilton Basin, strike approximately SW-NE and include Murihiku Terrane rocks lying to the east of the JMA (Figure 2). The original Waipa Fault of Kear (1960) incorporated the large eastwards deviation from the JMA to account for the separation of these two terranes. Hunt (1978) and Kirk (1991) suggested that this material is allochthonous, either through gravity sliding (Hunt (1978) or clockwise tectonic rotation linked to dextral shear along the terrane boundary (Kirk, 1991).

If the Hakarimata-Taupiri Ranges are an allochthonous block, then the Waipa Fault can continue to follow the JMA, and a separate boundary fault (Taupiri Fault) defines the northern boundary of the Hamilton Basin (Figure 2). As discussed further below, the potential fault zones located by this project within the Hamilton Basin align with the Hakarimata-Taupiri ranges and Taupiri Fault. Therefore, the displacement of the allochthonous block is likely to have played an important role in the development of faulting within the basement, but the nature of that role is not yet clear.

The compilation of the QMap Sheet 4 (Edbrooke, 2005), and the assessment of the potential for underground storage of CO₂ in the Waikato region (Edbrooke *et al*, 2009b; 2009b) resulted in the reassessment of a reasonable quantity of deep seismic and borehole data obtained during oil and gas exploration in the 1970s and coal resource surveys in the 1980s. This analysis provides useful interpretations of the basement structure and the older sedimentary sequences within the Hamilton Basin, indicating that the basement steps down towards the northwest with the greatest sediment thicknesses between Ngaruawahia and Whatawhata (Figure 3C). This contrasts with earlier interpretations. McLintock (1966) indicated a basement tilted towards the southeast, with the thickest sedimentary sequence occurring towards Cambridge (Figure 3a), while Lowe (1991) presented essentially uniformly thick sedimentary sequences within the basin, albeit with an alluvial fan infilling the hills in Karapiro Formation that was thickest around Cambridge.

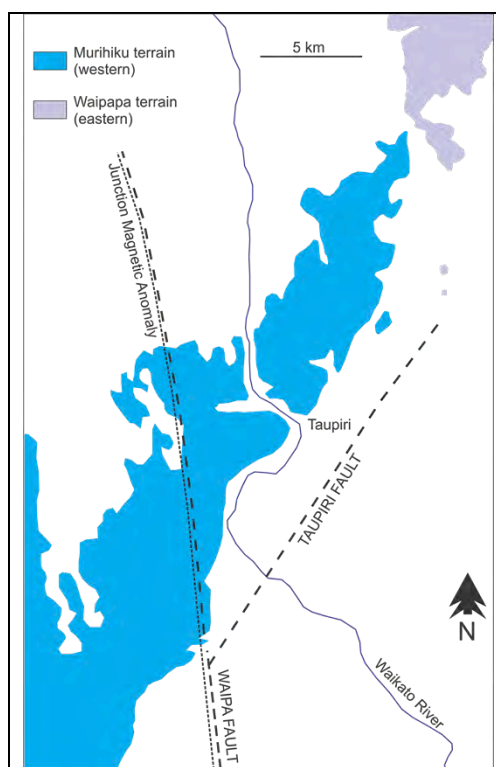


Figure 2. Hakarimata Range, basement terranes, and mapped faults at the northern limit of the Hamilton Basin.

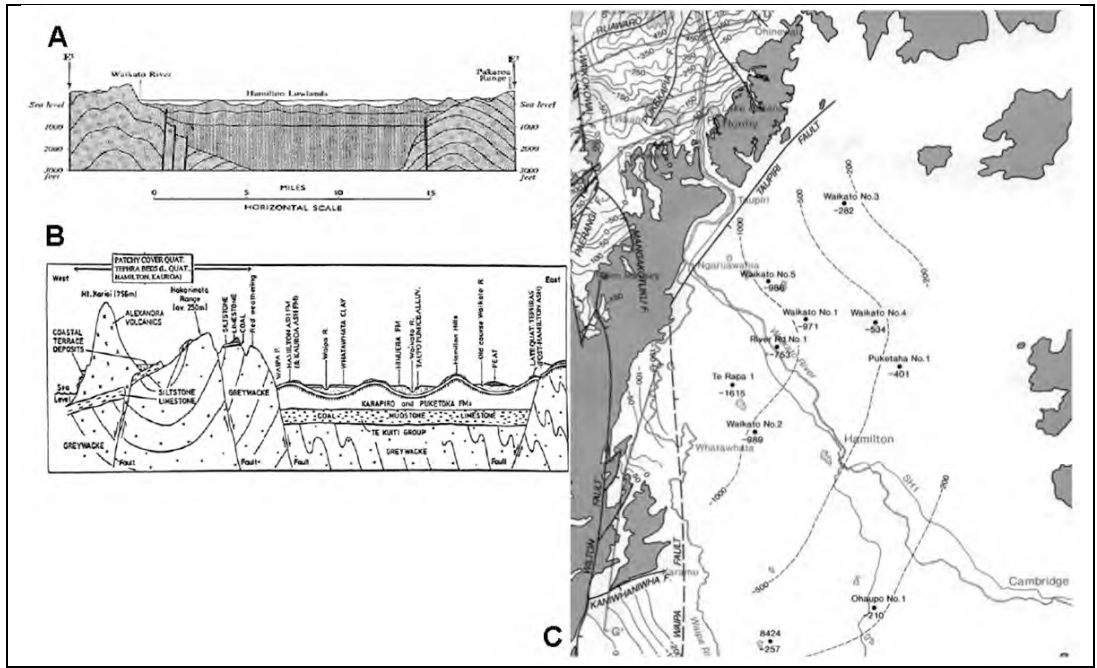


Figure 3. Alternative interpretations of the basement structure of the Hamilton Basin: A) McLintock (1966) cross-section from An Encyclopedia of New Zealand; B) Cross-section from an MSc thesis by Lowe (1991); and C) The approximate structure contours on basement and locations of test wells for oil and gas exploration for the northern Hamilton Basin (Figure 6.1, Edbrooke *et al*, 2009).

The oil exploration seismic data provided evidence for basement faults that extended into the sediments infilling the basin (Figure 4). However, the data were of poor quality and it was considered that insufficient data existed to extend the faults to the surface (Edbrooke, *pers. comm.*). However, the inferred fault to the east of the Kirikiriroa Stream coincides with the surface fault exposed in NE Hamilton, suggesting that surficial faulting within the Hamilton Basin may follow the basement structure.

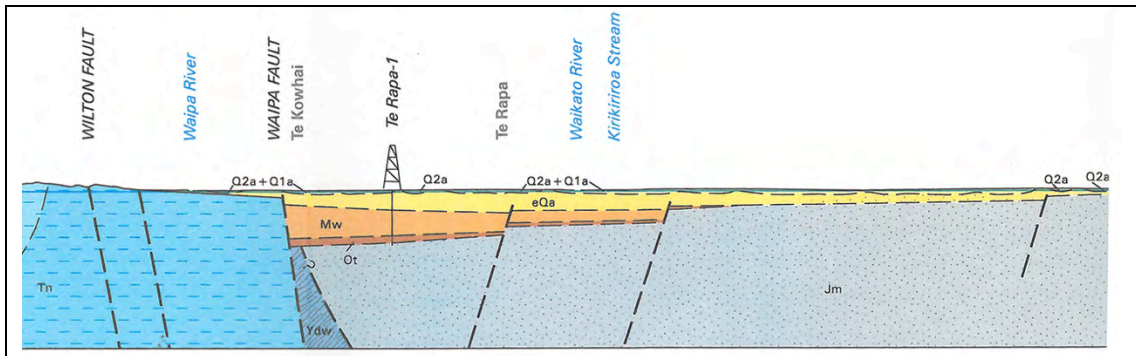


Figure 4. Cross-section through the Hamilton Basin from west to east through the Te Rapa-1 borehole (Figure 3) as depicted on QMap Sheet 4 (Edbrooke, 2005).

3.2 Gravity and aeromagnetics

A gravity map based on the Isostatic Residual Bouguer Anomaly developed by FrOG Tech (2011) is reproduced in Figure 5A. This indicates an area of low-density sediments infilling a deep basin in the northern part of the Hamilton Basin, abutting the Hakarimata Ranges. To the south towards Cambridge this negative anomaly steadily reduces, indicating basement closer to the surface consistent with the interpretation of Edbrooke *et al* (2009a) in Figure 3C.

The aeromagnetic image of MR4482 (Meyers, 2009) is reproduced as Figure 5B. The Junction Magnetic Anomaly (Waipa Fault) is clear at the western margin of the Hamilton Basin. The Alexandra Volcanics of Pirongia are also apparent on the western boundary of the Basin, with a few other magnetic features seen to the southwest of Hamilton City near Koromatua.

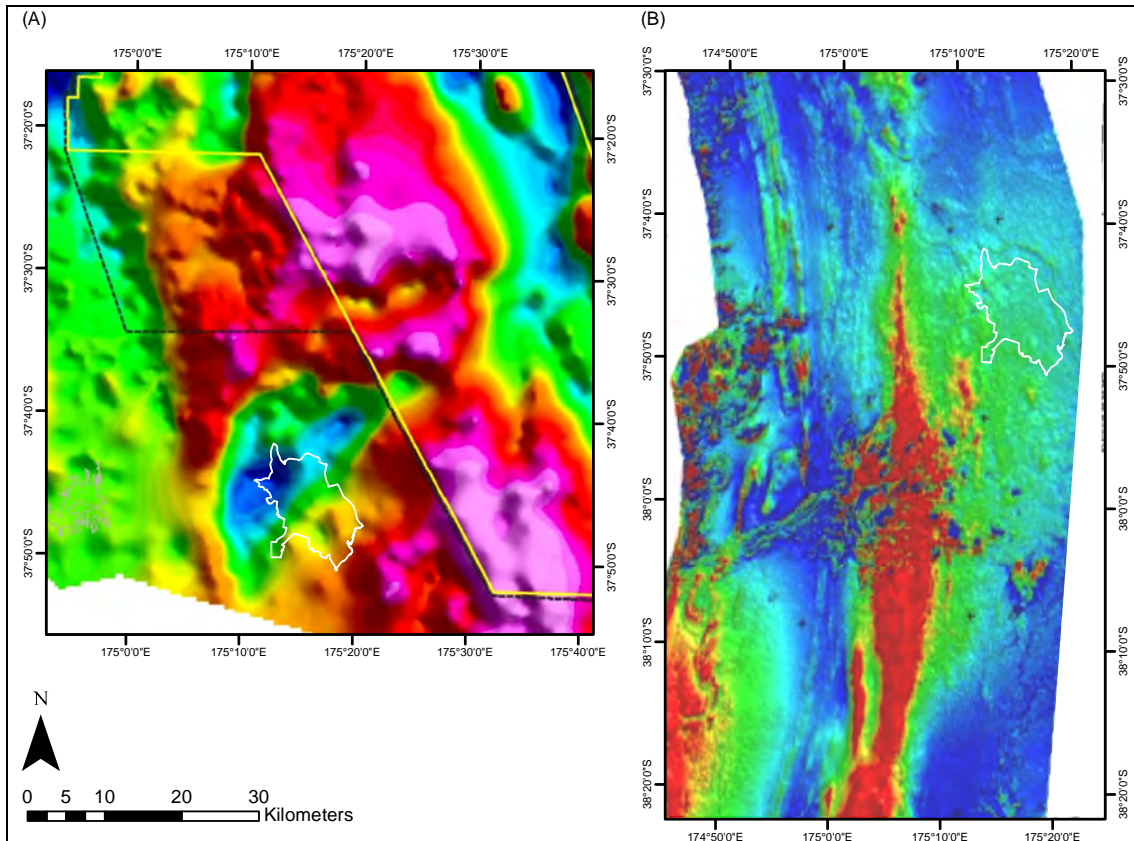


Figure 5. (A) Isostatic Residual Bouguer Anomaly map FrOG Tech (2011). (B) Total Magnetic Intensity map of Meyers (2009). Hamilton City is outlined on each map for reference. Note that neither original source gives quantitative ranges for colours, but in both cases blue is low and red is high.

4. Seismic Survey along Waikato River

4.1 Methods

On 29th March 2016 we undertook a shallow seismic reflection survey along the Waikato River from Cambridge to Taupiri, a distance of 56.25 km. A near continuous trace was obtained using a Knudsen Pinger chirp sub-bottom profiler (SBP) operated from the University of Waikato survey vessel *Taitimu*, with differential RTK GPS providing positional data. For this initial investigation we operated the Pinger at 3.5 kHz to achieve maximum penetration into the sub-bottom sediments, at the possible expense of some resolution, and with a 200 kHz transducer to track the bottom location (water depth). As noted in the proposal, previous investigations in loose alluvial sediments have found shallow seismic reflection to give poor results, so this low frequency was used to test if suitable reflections could be achieved. Due to the entrenched nature of the Waikato River within the southern area of the basin, the GPS system occasionally was unable to obtain a reliable fix. This was only significant immediately south of the Cobham Bridge, where the measured survey track appears to briefly deviate over land.

For the section of the survey between the Cambridge boat ramp and the Pukete boat ramp, an observer recorded changes in the geology exposed in the banks of the Waikato River. Between the Pukete Boat Ramp and the Taupiri Gap, fewer observations of riverbank geology were recorded. However, there were fewer exposures of the underlying geology for this section of the survey due to the lower relief of the riverbanks.

The seismic data obtained were examined using the Knudsen PostSurvey processing software, and a freeware package SeiSee. All the acquired profiles were initially assessed for quality, and 6 records were rejected because the data were poor quality due to experimentation with the SBP settings, or the record length was too short to identify features. All the locations of each seismic pulse were extracted as WGS-84 latitudes and longitudes, and converted to a Google Earth KML file to allow the survey track, and individual data file coverage, to be displayed in Google Earth. These data can also be imported into GIS.

The initial assessment of the seismic data also noted which data files contained apparent discontinuities in the sub-surface stratigraphy. These were checked to see if there had been any changes to the instrument settings, or accidental disruptions in the data recording. The settings used for the survey were determined by experimentation at Cambridge, and were left constant for the duration of the survey. Previous surveys had demonstrated that the processing software couldn't handle large data files, so the survey was deliberately broken into 10-minute long sections. However, the combination of a touch screen and bright sunlight meant that sometimes the data acquisition was turned off accidentally, or didn't turn on when it was supposed to. These periods can be identified by a larger gap between successive seismic profile locations than the surrounding data.

The data files identified as containing discontinuities were then processed by SeiSee, which has more tools available to filter and adjust the data than in PostSurvey. Sections of each file containing discontinuities or other features of interest were extracted, and the locations of these sections were also converted to a Google Earth KML file. The extracted sections were then interpreted, in conjunction with surficial geological data from 1:63,360 Geological Map sheets N56 (Ngaruawhia) and N65 (Hamilton), and side-scan and multibeam data acquired earlier by Wood (2006). An example of an interpreted section for the inferred Taupiri Fault, with geology, multibeam, sidescan, and Google Earth location is shown in Figure 6. The Wood (2006) study also includes 3D images of "scour holes" along the Waikato River (Figure 6). Some of these features do correlate with the sections with identified discontinuities, and these have been incorporated into the images in the Appendix A where appropriate.

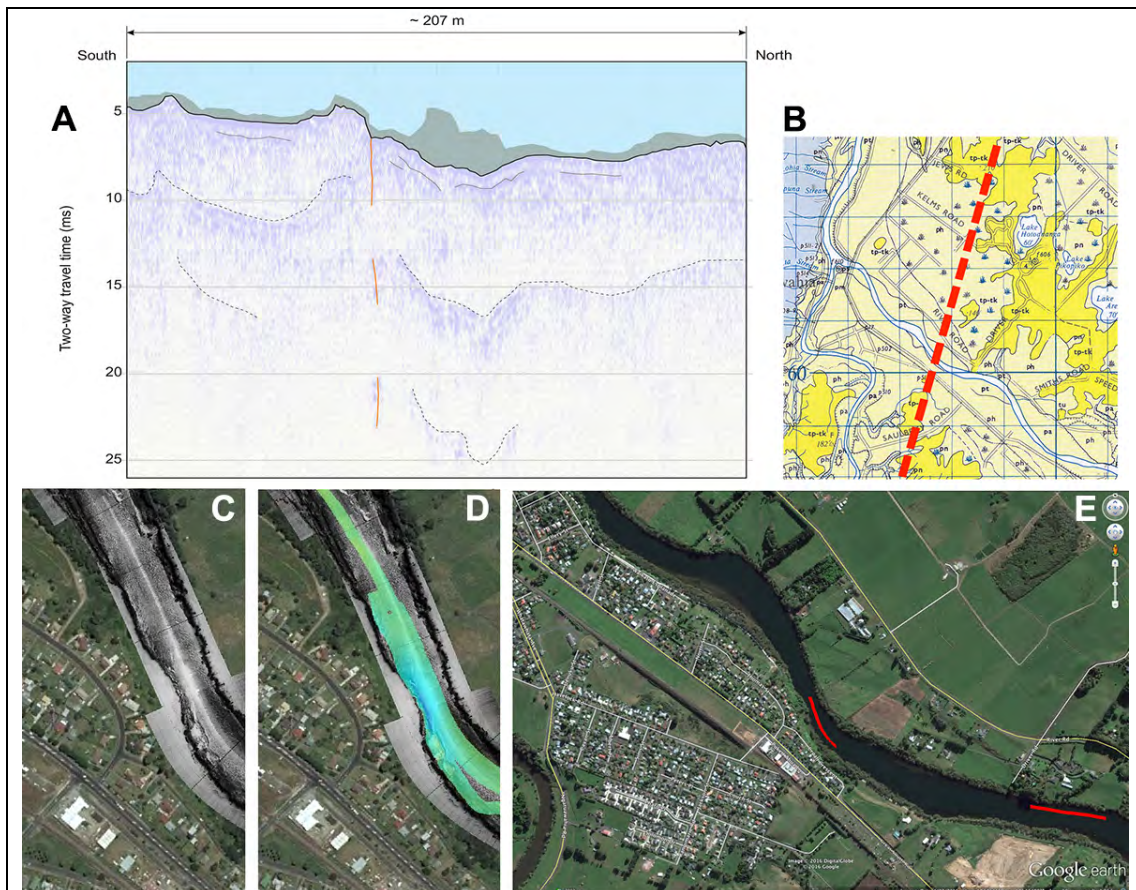


Figure 6: Interpretation of a seismic discontinuity assumed to be the Taupiri Fault. (A) Seismic reflection trace, (B) N56 surficial geology with inferred Taupiri Fault (Edbrooke et al, 2009), (C) sidescan image, (D) multibeam image, and (E) Google Earth location of the seismic section.

4.2 Results

The seismic survey proved successful at identifying apparent major discontinuities in the riverbed stratigraphy, with at least 25 zones of interest (Figure 7) where one or more steeply dipping reflectors is evident in the trace. These zones, with our initial interpretation of the traces and accompanying multi-beam and backscatter images, are summarised in Appendix

A. We cannot conclude that these are all necessarily faults, as erosional or depositional processes or interference from submerged objects such as trees may produce apparent steeply dipping features. However, during the seismic survey it was noted that several coincide with other evidence of faulting, including changes in the riverbank geology.

To assess if the methodology was detecting faults, the survey included areas where we expected to observe faulting associated with “known” faults depicted on QMap sheet 4. Specifically we targeted the Taupiri Fault at Ngaruawahia (Figure 6) and Taupiri (Figure A25). The following sections consider first the Taupiri Fault near Ngaruawahia as a confirmation, and secondly the other potential fault zones previously recognised (Figure 1).

4.2.1 Taupiri Fault near Ngaruawahia

The Taupiri Fault is an inferred fault that runs along the margin of the Hakarimata Ranges between Ngaruawahia and Taupiri (Edbrooke *et al.*, 2009). The inferred position of this fault coincides with location 1410-F1 (Appendix A – Figure A22) from our seismic survey (Figure 2), and is also marked by a “scour hole” and associated outcrop of resistant material in the multibeam record. Nearby sections with apparent discontinuities are possibly also associated with this fault system (eg. 1400-F1, Figure A21). This suggests that the maximum depth achieved by the seismic reflection survey may not be sufficient to identify a single main fault plane. Therefore, it was decided to define fault zones, containing one or more targets in relatively close proximity, which may represent splays of a single deep fault.

Based on the results for this location it was inferred that the seismic reflection survey undertaken was capable of detecting fault zones intersecting the Waikato River. However, the seismic survey did not locate any potential displacements in the vicinity of the two bridges across the river at Horotiu, where a fault is exposed in a cutting on River Road and geomorphic evidence of lateral spreading and terrace offsets suggests that a fault is present (Horotiu Fault, Figure 1). Therefore, it is considered that multiple lines of evidence are required to have confidence in the location of fault zones within the Hamilton Basin.

4.2.2 Previously proposed fault zones

Based on an initial analysis of LiDAR and geomorphic data, combined with the exposed fault zone in NE Hamilton City, three fault zones were suggested within Hamilton City (Figure 1): Kukutaruhe Fault Zone near the western boundary; Te Kourahi Fault Zone through the central City; and Te Tatua o Wairere Fault Zone near the eastern boundary.

The Kukutaruhe Fault Zone was based on the most lines of evidence, including the originally-identified exposed fault in a cutting, and the pattern of geothermal activity within the Waikato Basin. Subsequently the southern end of the fault zone depicted in Figure 1 was found to terminate in a small volcanic field at Koromatua. Two potential fault zones were located within the Waikato River that were associated with the Kukutaruhe Fault Zone: 1249_F1 Swarbrick Landing (Figure A14), which coincided with a sharp discontinuity in the geology exposed in the river bank that had been previously identified; and 1249_F2 Tauhara Drive

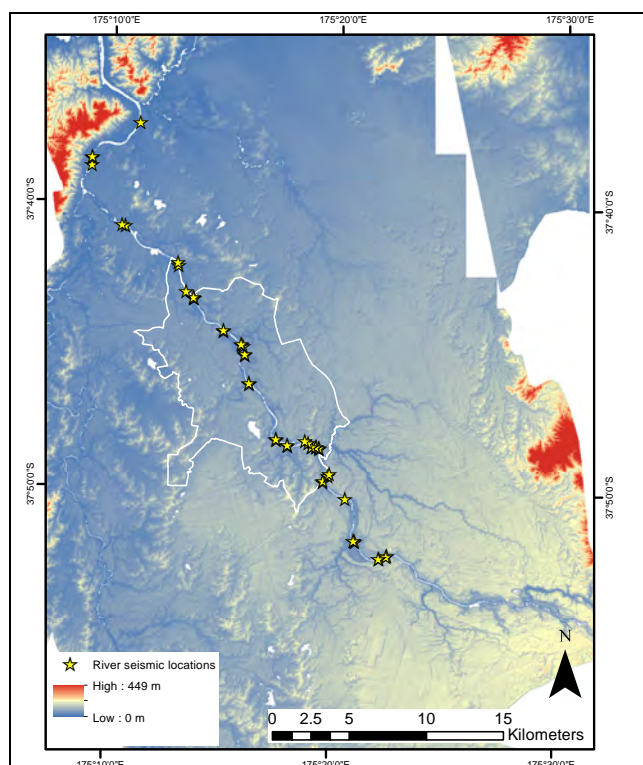


Figure 7. “Targets” identified in seismic reflection survey along the Waikato River as possible fault zones. The locations are overlain on a DEM of the area based on LiDAR data provided by Waikato Regional Council, and the boundary of Hamilton City is marked in white.

(Figure A15), which coincides with the Kirikiriroa Stream marked on the Qmap cross-section (Figure 4).

The Te Kourahi fault zone originally proposed in central Hamilton was not immediately identifiable in the seismic traces. However, a number of discontinuities that could be potential fault zones exist in the seismic traces between Cobham Drive and Claudelands Bridges; we have only included one (section 1216_F1 Graham Island) in Appendix A (Figure A12) as this appears the most likely to represent faulting. This zone is also in close proximity to exposures of Hinuera Formation containing liquefaction structures, which were observed in the 1970s (Hume, 1972; Sherwood, 1972; Hume *et al*, 1975). All of the identified discontinuities in this area need further investigation to determine if they do indeed represent fault zones.

The Te Tatua o Wairere Fault Zone along the eastern boundary of Hamilton City runs close to both the University of Waikato and the Hamilton Airport. The fault zone illustrated in Figure 1 is associated with fault zones within the riverbed at 1140-F1 (Figure A5), 1140-F2 (Figure A6), and 1153-F1 (Figure A7). A Summer Research Scholarship student, who undertook detailed geomorphic mapping and trialled the resistivity equipment, targeted the southern end of this zone, near Stubbs Rd. This work identified a possible correlation between fault zones crossing the Waikato River, and the existence of abandoned river channels incised into the Hinuera Surface above the present day river level. The results of this investigation are discussed in more detail below.

4.2.3 Additional Fault Zones

In addition to the previously identified fault zones, the seismic reflection data (Appendix A) suggest the presence of several other zones within the Hamilton Basin in close proximity to Hamilton City. In particular, zones that were considered for closer examination were found:

1. In the vicinity of Mystery Creek (Field-days Event Centre), including 1101-F1 Greywacke Hill (Figure A1) and 1101-F2 Mystery Creek (Figure A2);
2. Multiple discontinuities were identified between Silvia Crescent and the Hamilton Gardens, including Figures A7-A10, which includes the site for a proposed new river crossing to extend the Wairere Drive ring road system;
3. Between the Wairere Drive river crossing and the main sewer crossing between the two sides of Hamilton City at 1302-F2 Woodburn Ave (Figure A17); and
4. Near the Fonterra Dairy Factory in Te Rapa at 1326-F1 Osborne Rd (Figure A18).

To evaluate priorities for further investigation, existing data were re-examined and mapping of the geology and geomorphology along the Waikato River was undertaken.

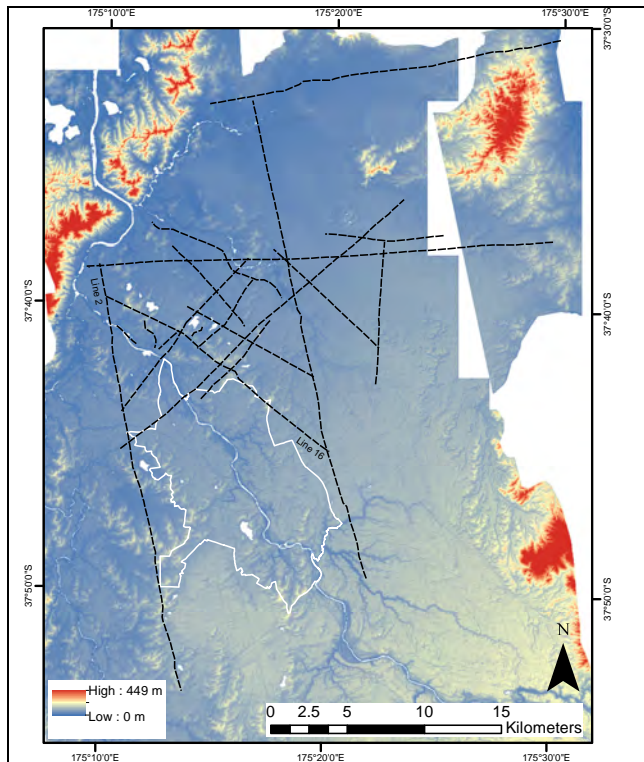


Figure 8. Seismic line coverage associated with PR569 (Liles, 1971). We have interpreted Line 2 on the western margin of Hamilton City, and Line 16 on the eastern side of the city in detail. The lines are overlain on a DEM of the region based on LiDAR data provided by Waikato Regional Council.

5. Existing Seismic Reflection Data

5.1 Methods

Seismic reflection exploration was undertaken in the early 1970s in the northern part of the Hamilton Basin. Data from these investigations are available from the NZ Petroleum and

Minerals website (www.nzpam.govt.nz) in the form of high resolution TIFF images related to PR569 (Liles, 1971). Twenty-four individual lines are available, covering the part of the Hamilton Basin from Hamilton City northwards (Figure 8). No original data are available, and the TIFF files represent images of raw data output without significant post-processing. Interpretation of these lines was undertaken manually on the TIFF images. The data quality is thus limited and interpretation somewhat subjective, especially in regions of poor signal return.

We have at this stage considered two key lines: PR569-2 and PR569-16 as these two long lines run approximately north-south through the basin and thus intersect the inferred faults at the most acute angle.

Gravity (FrOG Tech, 2011) and aeromagnetic (Meyers, 2009) data are also available from the NZ Petroleum and Minerals website. These data are images only and were georeferenced to our ArcGIS files.

5.2 Results

Summary images of lines PR569-2 and PR569-16 are presented in Figure 10A and 10B. These images show the uninterpreted section at the base, the interpretation overlaid in the middle, and the interpreted structure presented at the top along with a topographic profile derived from LiDAR data provided by Waikato Regional Council. A coloured strip indicates the surficial geology along the profile, and some locations are marked for reference. PR569-2 intersects the location of a well log presented by Liles (1971), which allows correlation of two key stratigraphic boundaries: the base of the Tauranga Group sediments and the top of the greywacke basement.

Many faults are inferred from these profiles (Figure 9), and there is good agreement between recognized faults and their geomorphic expression in the topographic profile. The faults recognised are steeply dipping in the shallow stratigraphic sequence: most are normal faults dipping toward the south, often associated with antithetic normal faults dipping northwards or small reverse faults. The quality of the data means that reliable measurements of offset cannot be obtained.

The basement surface mapped in PR569-2 indicates a steep dip in the north on moving away from the Hakarimata Range, falling to a maximum under northern Hamilton, then rising at a gentle slope ($\sim 3^\circ$) towards the south. This agrees with the gravity anomaly presented by FrOG Tech (2011) as indicated in coloured strip in Figure 10A. As the seismic reflection data is very poor below the greywacke upper surface, it is unclear whether or not the faults continue into the basement, but we assume that they do.

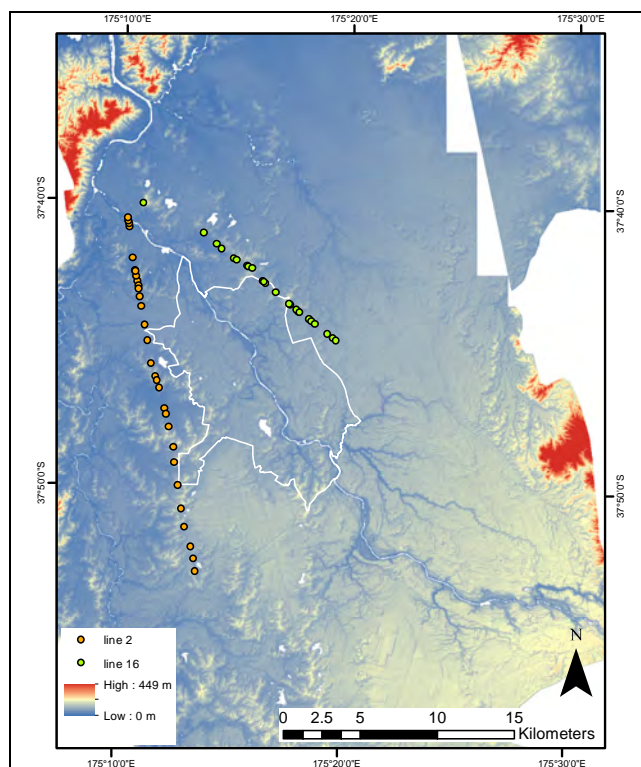


Figure 9. Locations of faults recognised on seismic lines 2 and 16 of Liles (1971) as indicated on Figure 10. Positions of the uppermost identifiable trace of the fault in the seismic images are extrapolated to the surface.

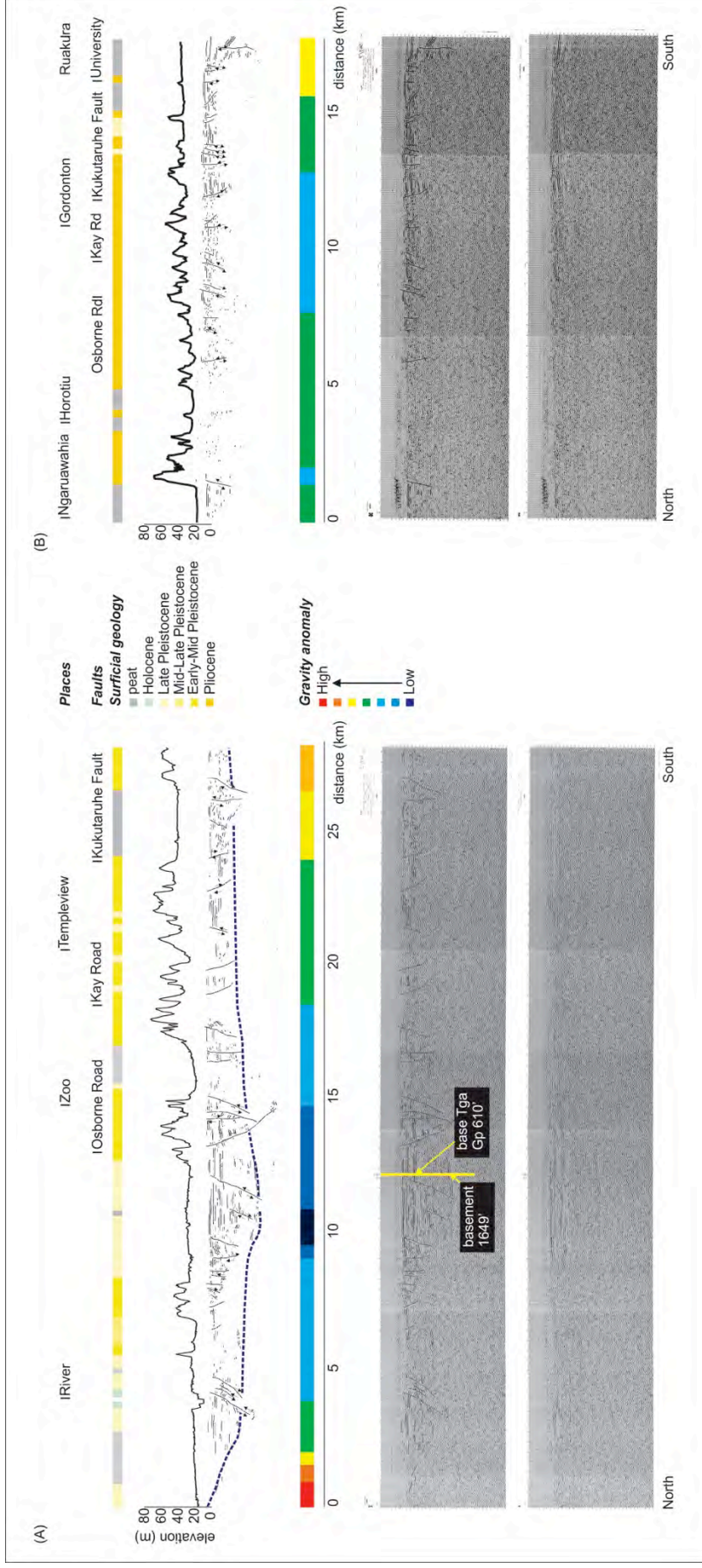


Figure 10. Interpretation of seismic reflection lines from PR569 (Liles, 1971). (A) Line PR569-2 running along the western margin of Hamilton City. (B) Line PR569-16 running to the east of Hamilton City. Original and interpreted images are shown at the base of the diagrams, with key stratigraphic horizons identified from borehole Te Rapa-1 (Liles, 1971) marked on (A). Indicative gravity anomaly strips are shown, with colours derived from FrOG Tech (2011). Interpreted sections, including depth to basement for (A) marked with a dashed blue line are overlain with geomorphology (vertical exaggeration ~ 30x), and surficial geology is marked with a coloured strip. Fault traces identified on land are indicated, and several geographic locations are projected onto the line and marked for reference.

6. Mapping riverbank geology

6.1 Methods

Riverbank geology has been mapped using standard geological mapping techniques. Two boat trips were undertaken on 13 December 2016 and 23 March 2017, during which the riverbank geology was mapped from the Narrows Bridge (37° 50' 30.7" S, 175° 20' 54.2") to the old Horotiu Bridge (37° 41' 52.1" S, 175° 12' 19.9" E). Additional mapping along the riverbanks has been undertaken from the land during the summer of 2016/17.

In all cases we attempted to classify materials by published stratigraphic units (Heron 2014; Edbrooke 2005), but in many instances recognition of unit was not possible due to limitations of the exposures. Thus, ignimbrites are grouped as just a broad classification at this stage, and classes of undifferentiated Holocene or Pleistocene sediments are included. Thin sections are currently being prepared and described to refine the classification of many units. On the basis of field observations and comparison of outcrop patterns, several faults have been tentatively identified.

6.2 Results

Figure 11 presents our current outcrop map for the riverbanks survey. Surprisingly little clearly identifiable "Hinuera Formation" material was exposed along the riverbanks in this area, though this is likely a function of vegetation and development patterns. As the Hinuera Formation forms shallow-angle (compared with other materials) slopes with unconsolidated sediment, vegetation growth on this material is extensive and hence obscures direct observation of the geology. Hinuera Formation is mapped in Hamilton City on the eastern bank of the river from Cobham Bridge to the Claudelands Bridge. It likely occupies considerably more of the channel margins through the city portion of the map than indicated in Figure 11.

Ignimbrites of Walton Subgroup (Pliocene – mid Pleistocene) age are readily identified in outcrops near the Hamilton Gardens and in a gully at the southern boundary of the city near Stubbs Road. Throughout this region, stratigraphic relationships between the ignimbrites and surrounding materials are indicative of faulted contacts, but only one direct exposure of a contact was identified (discussed below). Other materials of Walton Subgroup age are plotted as "Undifferentiated Pleistocene Sediments"; it is not clear whether or not these are sediments or reworked pyroclastic materials; thin sections are being prepared to help elucidate this.

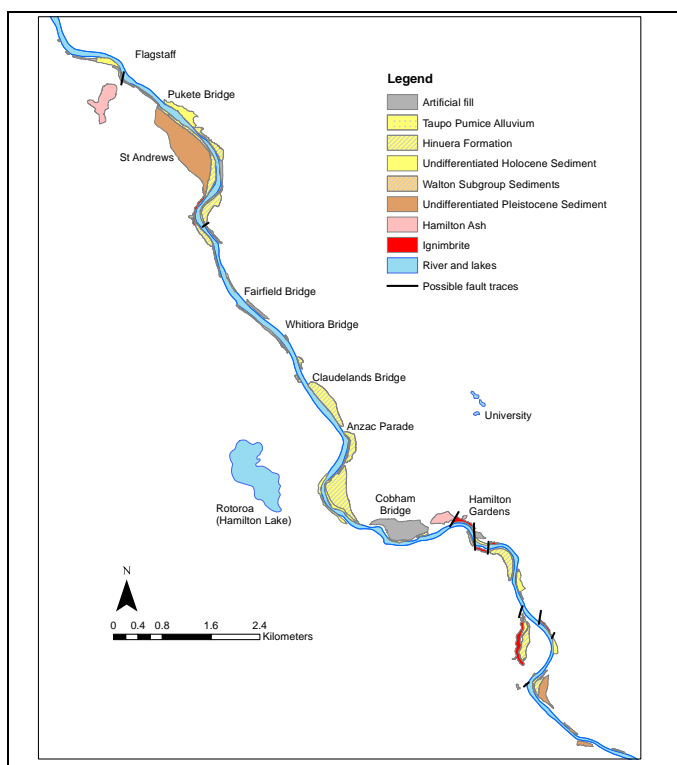


Figure 11. Current geological map of river bank outcrops along the Waikato River channel between the Narrows and old Horotiu bridges.

7. Resistivity

7.1 Methods

Electrical resistivity surveys have been undertaken at 4 sites (Table 1): Kerepehi Fault near Te Poi; Stubbs Road near Hamilton airport; Osborne Road near the NW boundary of Hamilton; and the Inland Port site, Ruakura, close to the University of Waikato.

Table 1. Test conditions for electrical resistivity surveys. Note that the end=point values for ILPORT3 were considered inaccurate so this line was excluded from the model.

Location	array type	line no.	start	finish	spacing (m)
Kerepehi	Dipole-dipole	KERE1	N5816988 E1845098	N5816996 E1845561	20
Stubbs Rd	Dipole-dipole	STUBBS1	N5810660 E1804586	N5810993 E1824729	13
Osborne Rd	Dipole-dipole	OSBRN1	N5824506 E1797158	N5824516 E1797084	3
		OSBRN2	N5825586 E1797160	N5824510 E1797083	3
		OSBRN3	N5824481 E1797160	N5824502 E1797082	3
		OSBRN4	N5824477 E1797158	N5824500 E1797079	3
Ruakura	Dipole-dipole	ILPORT1	N5816024 E1804343	N5815805 E1804497	8
		ILPORT2	N5816031 E1804355	N5815810 E1804511	8
		ILPORT3	N5816037 E1804364	N5815812 E1804519	8
		ILPORT4	N5816046 E1804371	N5815824 E1804528	8

Initially, 2-dimensional profiles were undertaken across a known trace of the Kerepehi Fault, an active fault recognised in the Hauraki Basin. This fault displaces a slightly older phase of the Hinuera Formation than that which is in the Hamilton Basin (Manville and Wilson, 2004), and is known to have moved several times during the Holocene (Persaud *et al*, 2016). This site was used to identify the signal produced by a fault trace in these materials. Two-dimensional profiles were undertaken at a site near Stubbs Road at the southern boundary of Hamilton City. The 3-dimensional capability of the equipment was then employed at Osborne Road and the Inland Port location.

An AGI Supersting8 electrical resistivity meter with 20 m electrode spacing was used for resistivity surveying. The following equipment settings were standard for all surveys:

- Cycles: 2
- Max error: 2.0
- Max repeat: 1
- Max current: 1250mA
- Measure time: 1.2 s
- Separate potential: OFF
- Measure mode: RES
- Single – step cmd lines: OFF

Other test conditions specific to each site are outlined in Table 1.

The results for the Kerepehi Fault site will be presented in this section, while the results from the other locations will be presented in Section 8 as specific sites are discussed.

7.2 Kerepehi Fault

A trial of the resistivity system was conducted on the Te Poi segment of the Kerepehi Fault close to the Madill Trench site reported by Persaud *et al* (2016). Their interpreted trench log for this site is shown in Figure 12.

The Kerepehi Fault was imaged at 20 m electrode spacing for a length of 480 m. Only a single two-dimensional profile was undertaken at this site, primarily as a test of the equipment. Note that this section was undertaken with a relatively wide spacing and long line length to obtain maximum depth of penetration, which means that the profile is consequently of low resolution (Figure 13). Therefore, it is not possible to directly compare the results of the resistivity survey with the stratigraphic units within the top 6 m reported for the Madill Trench site.

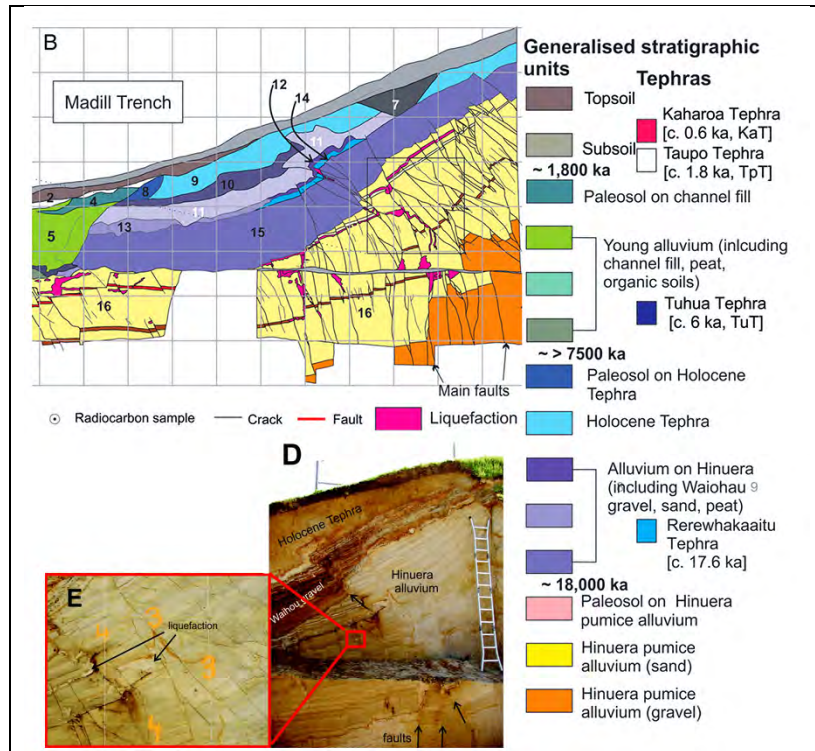


Figure 12. Interpreted log and images of the Madill Trench through the Te Poi segment of the Kerepehi Fault within the Hauraki Basin presented by Persaud *et al* (2016) in their Figures 5, S3 and S5. (B) Madill Trench Log. (D) Photo of exposed face of trench with 4 m ladder for scale. (E) Enlargement of complex faulting pattern with some evidence of liquefaction.

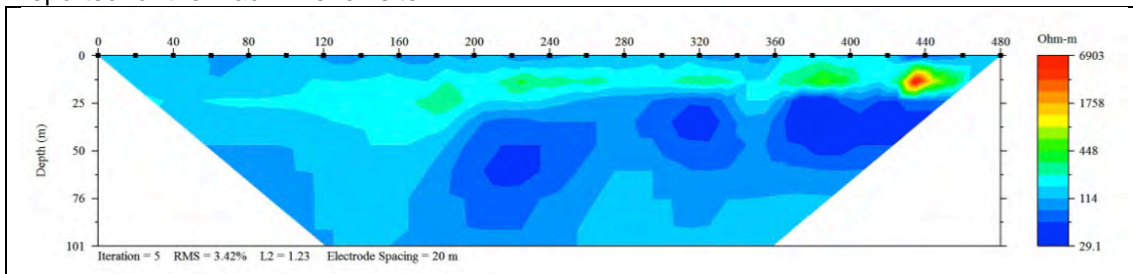


Figure 13. Inverted resistivity cross-section of the Te Poi segment of the Kerepehi Fault close to the Madill Trench section (Figure 12). The section runs west-east and intersects the surface trace of the fault at approximately 180 m.

However, it is possible to assess if the deeper stratigraphy shows evidence of fault displacements of underlying units as suggested by Houghton and Cuthbertson (1989) in Figure 14. Their analysis of available data suggests that the Kerepehi Fault offsets the Waiteariki Igneimbrite underlying the Hinuera Formation within the Tauranga Group sequence. The inverted resistivity

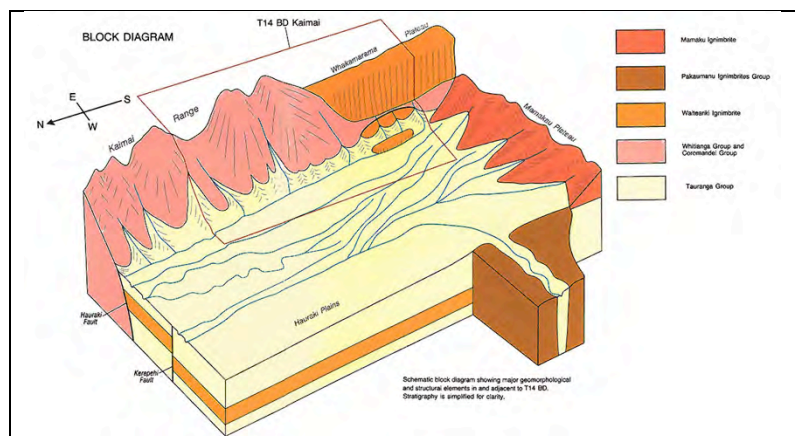


Figure 14. Block diagram of the inferred stratigraphy of the southern Hauraki Basin (Houghton and Cuthbertson, 1989).

section (Figure 13) across the Kerepehi Fault scarp shows a low RMS error of 3.4 %, indicating a good fit between the measured and modelled results, though L2 (> 1.0) suggests incomplete convergence to an ideal solution.

The interpreted range of resistivity is 29–6903 Ω m, with overall a zone of higher resistivity (> 200 Ω .m) overlying lower resistivity materials (< 100 Ω .m). The surface materials in the Te Poi area are largely gravels and sands of the Hinuera Formation, and the higher resistivity materials in the upper 25 m of the profile fit well with this interpretation. Lower resistivity below ~25 m suggests more clay-rich materials, which is consistent with weathered Waiteariki Ignimbrite (Figure 14) that outcrops at the surface at Okauia north of Te Poi. At a distance of ~180 m from the start of the transect the surface trace of the Kerepehi Fault is intersected, with uplift to the east. In the inverted resistivity section the dark blue representing the low-resistivity weathered ignimbrite disappears, suggesting uplift of this material to the east in keeping with the surface trace evidence and the model of Houghton and Cuthbertson (1989). We also undertook a further test of the equipment at the base of one of the Hamilton Hills within the grounds of Waikato University (Figure 15), using the dipole-dipole gradient method with 1 m electrode spacings. These settings reduced the penetration depth, but increased the resolution. At this location the Hamilton Ash beds are dipping underneath the Hinuera Formation, which consists of braided river deposits forming low ridges (levees) that separate coarser channel deposits (Horotiu soils) and finer interfluvial deposits that grade from Brunwood Soils on the higher elevations into Te Kowhai Soils in the hollows. The Hamilton Ash beds have larger clay content than the units within the Hinuera Formation and have < 60 Ω .m resistivity. The gravelly channel deposits have a resistivity > 225 Ω .m, with the remaining units lying in the range 60-225 Ω .m.

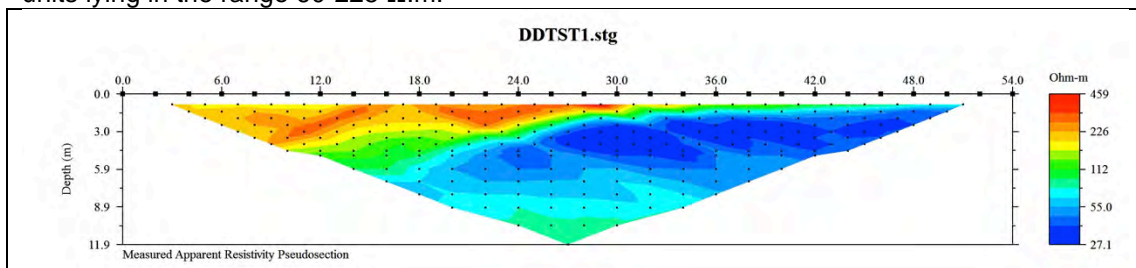


Figure 15. Resistivity survey across the boundary between the Hamilton Hills and Hinuera Surface within the grounds of the University of Waikato, Hamilton.

8. Identified fault zones

Six on-land sites (Figure 16) were identified through field mapping following the seismic reflection survey, riverbank mapping, and within excavations for the Waikato Expressway and other infrastructure. These have been investigated through geological and geomorphological mapping, together with resistivity surveying where appropriate.

These sites were used to define three fault zones that have been examined further. The results of the detailed examinations are discussed below.

8.1 Kukutaruhe Fault Zone

The Kukutaruhe Fault Zone was the first recognised, leading to this project. We currently have two near-surface exposures of faulting within this fault zone.

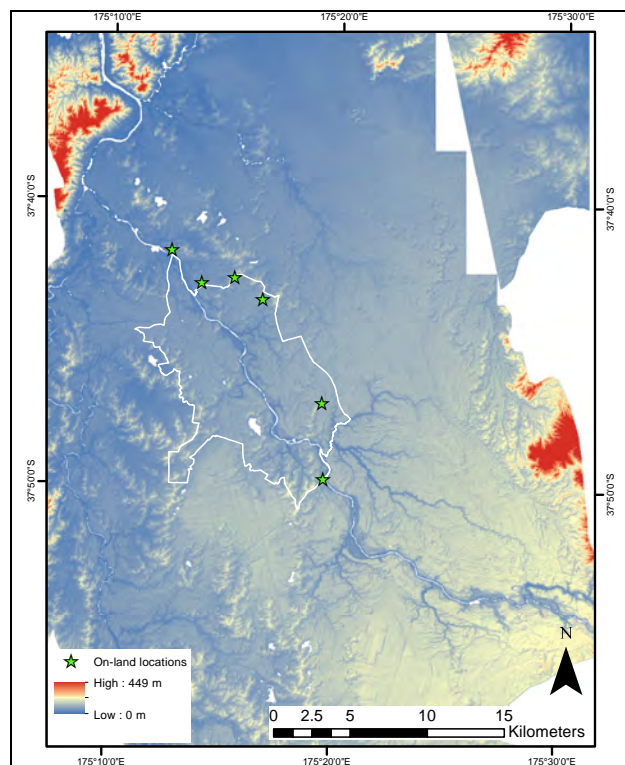


Figure 16. Locations of fault traces identified from outcrop or cuttings.

8.1.1 Cutting near Rototuna

The site initially identified at Rototuna (37°43'24" S, 175°16'40" E) is a fault zone exposed in the wall of an excavation (Figure 17). The zone is approximately 4 m wide, comprising 4 main strands of the fault trace, with several smaller strands linking between them, and has a total vertical offset across the zone of approximately 0.5 m. Normal (extensional) movement occurs across this zone, with dips on the strands ranging from 51 – 84°. The 4 apparent main strands have an average dip direction of 089° (strike 356°), while the 2 measurable minor strands have a dip direction of 351° (strike 081°).



Figure 17. Exposed face within an excavation at Rototuna showing faults within the Kukutaruhe Fault Zone.

Unfortunately, the top layers of the stratigraphy were removed during excavation, so limited stratigraphic information is available to date the movement of this fault. The white layers at the top of the cutting, which are clearly displaced by the fault movement, are tentatively identified as K12/K13 (Kauroa ash sequence, likely Ongatiti Ignimbrite correlative) of approximately 1.23 million years. Soil infilling down the fault traces is identified as part of the Hamilton Ash sequence, being amongst the younger portion due to the strong brown colouration (the oldest Hamilton Ash units are pale coloured). This suggests that the fault movement is within the last 250,000 years, but this is not definitive.

From this exposure in Rototuna, inspection of the geomorphology using LiDAR shows a sharp ridge running SW-NE through the Hamilton Basin, approximately coinciding with the southern margin of the basement low identified in the gravitational anomaly (FrOGTech, 2011). This ridge is uplifted to the north and down-dropped to the south as a normal fault, indicating extensional movement as exposed in the Rototuna site. The ridge also corresponds with areas of known elevated geothermal water temperatures, and crosses the river at a series of sharp right-angle bends near Day's Park and St Andrew's Golf Course.

The inferred fault zone coincides with seismic section 1249_F1 near Swarbrick Landing (Figure 18, Figure A14), and ridges of resistant material associated with "scour holes" identified previously by Wood (2006) as shown by multibeam data (Figure A15) at a second, nearby "target" in the seismic profile (1249_F2) that is likely part of the same fault zone.

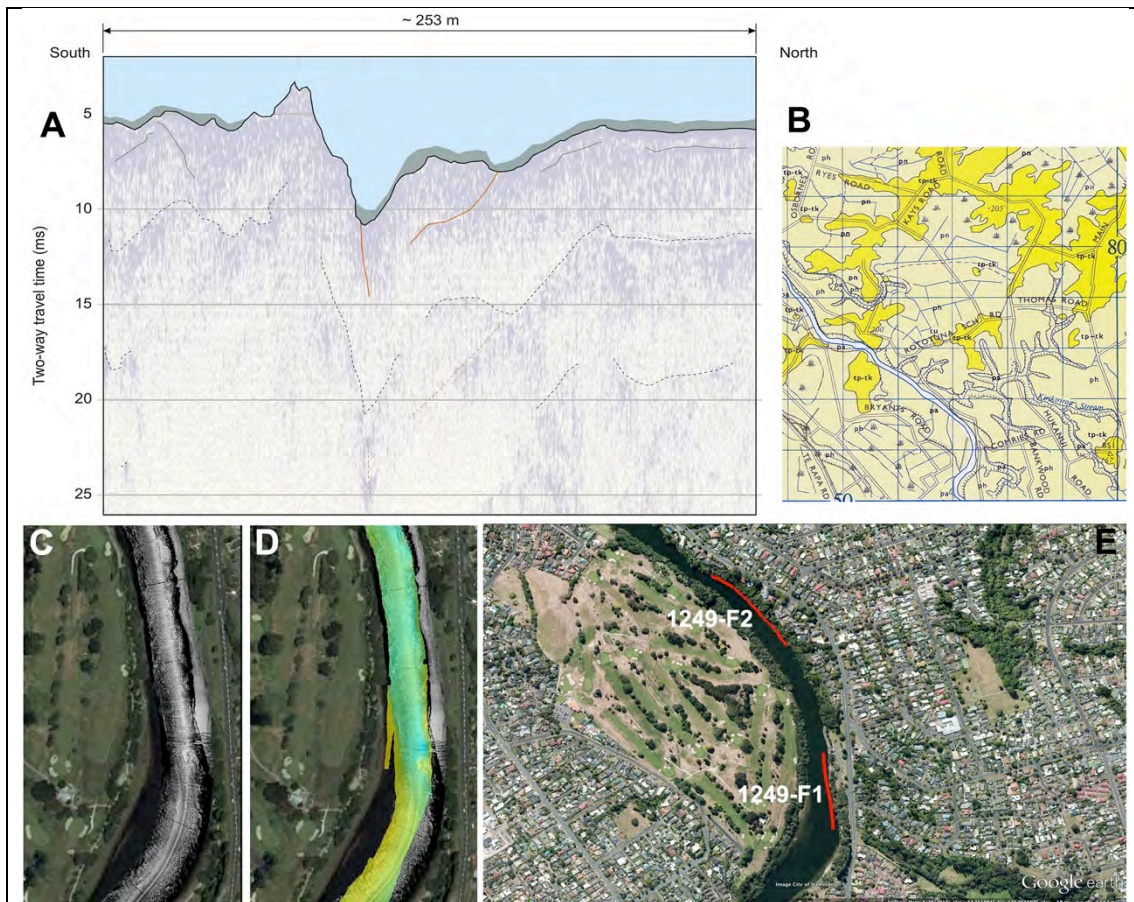


Figure 18. Kukutaruhe fault zone observed within the Waikato River bed. (A) Seismic section showing multiple discontinuities below the riverbed near Swarbrick Landing in section 1249-F1 – the low-angle trace may reflect the fact that the river is running parallel to the fault for part of this section, (B) N56 surficial geology, (C) sidescan image, (D) multibeam image, and (E) Google Earth locations.

8.1.2 Kay Road Cutting

Recent cuttings created as part of the Hamilton Bypass portion of the Waikato Expressway development have exposed a complex fault zone within the hill section at Kay Road on the northern boundary of Hamilton City (37°42'40" S, 175°15'25" E). This site consists of a deep cutting through a hill, with the cutting running approximately normal to the strike of the ridgeline. Thus two exposures exist, one on each side of the excavation. The exposure on the southwestern side (Figure 19B) consists of an approximately 85 m long by 35 m high embankment, while the exposure on the northeastern side (Figure 19A) is approximately 70 m long by 30 m high.

These cuttings expose a complex fault zone with numerous steeply dipping normal faults, together with apparently lower angle linking strands. Dip and strike measurements on inferred fault surfaces fall into two main sets with orientations 197/72 (strike/dip °T) and 099/07 °T. Most measurements fall into the first set (10 of 18) and this is the dominant strike direction for the steeply dipping faults exposed in the cutting. Fewer, shallow-angle faults seem to accommodate some of the movement in the graben areas developed by slip along the steep faults. We are still undertaking modelling of this fault system to better understand the relationships between individual strands identified.

These complex faults offset sedimentary Walton Subgroup materials in the lower portions of the section, and the Kauroa Ash materials above them. Apparent vertical offsets up to 8.5 m on individual faults are measured. However, no evidence could be found for displacement of the distinctive Rangitawa Ash at the base of the Hamilton Ash Sequence (shown in pale in images). This unit is dated at approximately 350,000 years (Lowe et al., 1991), so movement on these faults occurred before this time.

While a complex fault zone with large offset, it is difficult to trace this fault geomorphically for much distance across the basin, however it would appear to correspond to 1302-F1 and

1302-F2 Woodburn Ave seismic reflection targets (Figures A16 and A17), indicating that this fault converges towards the fault exposed in Rototuna. Therefore, we consider that both are splinters of the Kukuraruhe Fault Zone, and form a more continuous fault zone slightly to the south of where they are recognised in the east of Hamilton. The difficulty tracing this fault may reflect the age of the last movement, as geomorphic processes will have had the time to alter the evidence considerably.

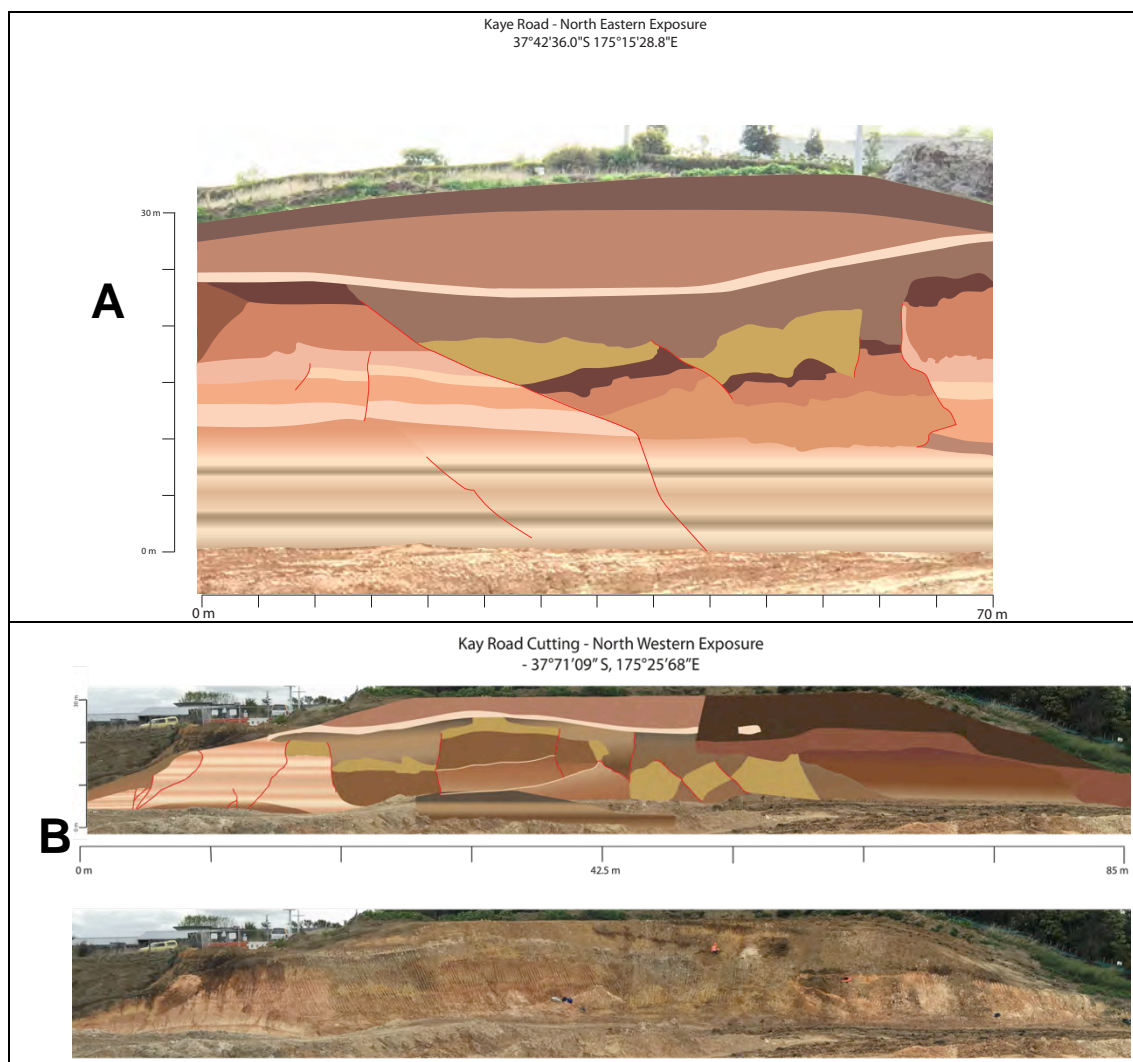


Figure 19. Interpreted stratigraphy of the (A) northeastern and (B) southwestern side walls of the cutting through Kay Rd for the Hamilton Section of the Waikato Expressway. The lowest image in (B) shows the exposed face for comparison.

8.1.3 Synthesis

We infer that the Kukuraruhe Fault Zone is the most continuous fault zone and can be traced from geomorphic evidence across the basin from near Te Awamutu in the southwest to north of Hamilton City in the northeast. Displacement along this zone is responsible for the almost continuous ridge from Te Awamutu, through Ohaupo and Templeview, to Koromatua (Figure 20). Two seismic reflection targets near Day's Park in Hamilton indicate points at which the main fault and Rototuna splinter cross the Waikato River, and a further two to the north represent the fault zone identified at Kay Road. The coincidence of the main lineation with the southern margin of the deep basin revealed in the gravity data (Figure 5) suggests that it is a deep-seated structure, consistent with the inferred basement fault in the QMap cross-section (Figure 4).

Contrary to the basement gravity low, which suggests down-dropping to the north at this point, the surface trace indicates relative uplift to the north and down-dropping to the south. From the ground surface profile included on Figure 20, it is also apparent that the hills formed

along the main fault and the splinters have a steep face dipping towards the south and a much gentler slope dipping towards the north. This geomorphology is common to many of the hills within the Hamilton Basin. It is suggestive of a listric nature to the faults, which will be discussed further in Section 10.

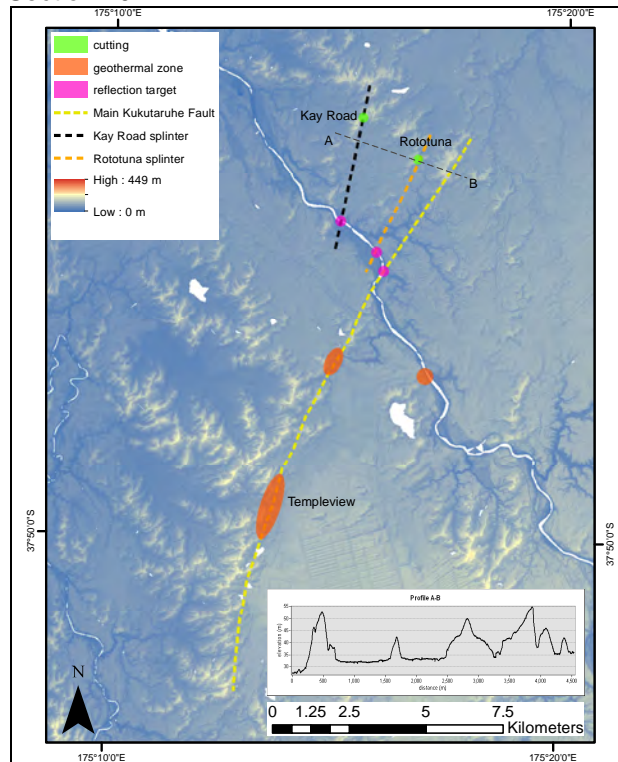


Figure 20. Kakataruhe Fault zone showing inferred main fault based on LiDAR elevation model together with two splinters with exposures at Rototuna and Kay Road (discussed below). A surface profile along line A – B intersecting the three faults is included.

8.2 Te Tatua o Wairere Fault Zone

Seismic reflection along the river indicated a distinctive zone near Stubbs Road at the southern boundary of Hamilton City (1140-F1, Figure A5). This coincided with the small fault identified in the riverbank geological survey, together with geomorphic features recognised from perusal of the LiDAR images, which suggested disruption of the river terraces in this area. Further analysis of this site was undertaken including geological and geomorphological mapping and 2D resistivity surveys.

The same zone was evident within the riverbed between Stubbs Rd and the proposed location of a bridge extending Wairere Drive to the southwest of Cobham Drive, with multiple fault targets at 1140-F2, 1153-F1, 1159-F1, 1159-F2 and 1159-F3 (Figures A6-A10). Further, LiDAR and resistivity survey data at the site being developed for an Inland Port adjacent to the University of Waikato indicate the same zone extends north-eastwards from the University of Waikato Campus.

8.2.1 Stubbs Road

The southern end of the fault zone at Stubbs Rd was the first area investigated as a preliminary survey indicated that there may be geomorphological features in the terraces flanking the river associated with fault movement. A Summer Research Scholarship student undertook an investigation combining field mapping, GIS analysis of the LiDAR data and resistivity surveying. A MSc student funded by the Waikato Regional Council subsequently undertook detailed geological mapping of the area, including an examination by boat of the exposures along the river bank.

8.2.1.1 Geomorphology and geology

The geomorphology at this site consists of a north – south trending set of hills, which disappear into peat swamps to the north and south. The Waikato River appears to turn sharply to the northeast at Stubbs Rd, and more gently to the northwest closer to Hamilton City (Figure 21). There are terraces flanking the river on the upstream side approaching the bend. While some continue around the bend, the pattern of terraces appears to be disrupted. Above the river on the western bank there is a deep channel (50-100 m wide) that initially follows the alignment of the upstream river channel, before turning towards the north. This has been interpreted as an abandoned river channel.

A gully system containing a small stream enters the river at the sharp bend, and the system generally aligns with the river channel downstream of the bend (Figure 21). This type of gully/stream system has been classified as an insequent stream forming randomly, albeit with a dendritic pattern, by headward erosion within horizontally stratified relatively homogeneous materials (Schofield, 1965).

However, the relationship between the gully system and the other features at Stubbs Rd suggests that at least some of the gully/stream systems within the Hamilton Basin are influenced by non-homogenous materials affected by faulting, resulting in subsequent or resequent streams following the definitions of Morisawa (1968). Geological mapping located ignimbrite along the margin of the upstanding hills and the left bank of the elevated abandoned channel; Late Pleistocene Hinuera Formation was mapped on the upper levels of the right bank of the former river channel. Younger (Late to Mid- Pleistocene?) sediments and volcanoclastics comprise the modern riverbank deposits in the area. These materials are sufficiently resistant to form a waterfall within the stream discharging into the Waikato River at this site.

A fault (Figure 22) with orientation 137/85 (strike/dip, °T) was mapped at 37° 49' 39.0" S, 175° 19' 35.2" E; this is marked on the map in Figure 16. This fault offset shallow-dipping sedimentary beds at the base of the sequence, and was marked by ductile deformation of a

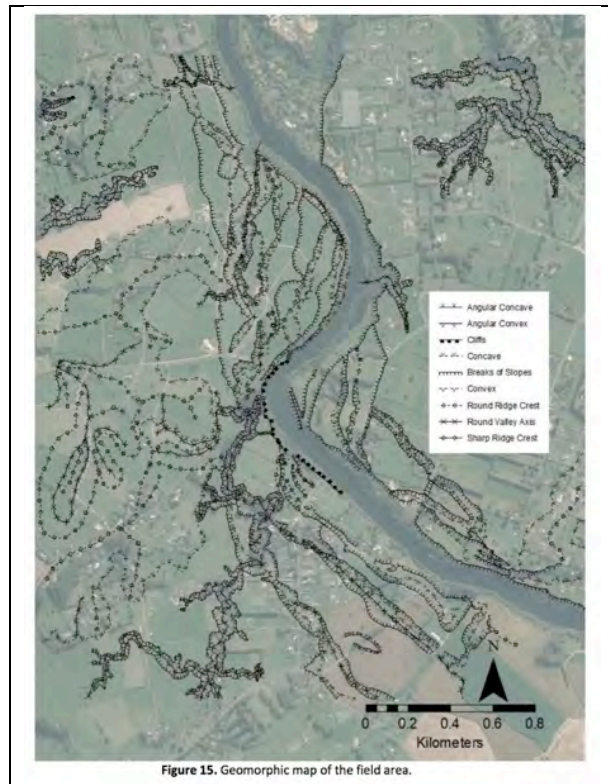


Figure 15. Geomorphological map of the field area.

Figure 21. Geomorphological map of the Stubbs Rd area (M Cummins project report).

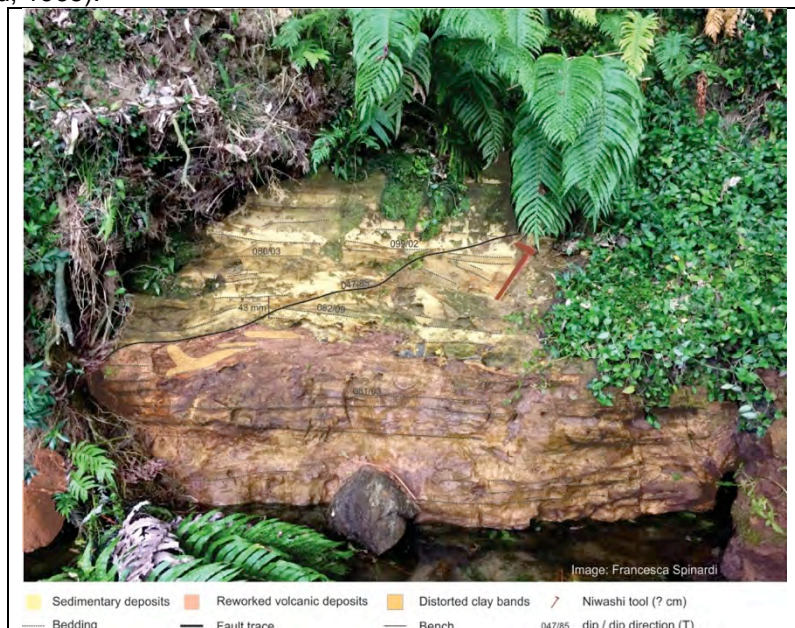


Figure 22. Fault exposed at Stubbs Rd with an orientation of 85/047 (dip/dip direction, °T).

pale yellow clay layer, together with iron staining on the fault surface. The measured apparent vertical offset at this site was 43 mm. The location and orientation of the mapped fault is consistent with the features in the riverbed from seismic reflection survey and earlier multibeam data.

8.2.1.2 Resistivity

A two-dimensional resistivity survey was undertaken at Stubbs Road. The position of the lines was aimed to target the fault zone identified in the seismic survey and intersect the abandoned channel inferred from the geomorphology (Figure 23).

The results of the resistivity survey (Figure 24) show patterns similar to those observed for the Kerepehi Fault, indicative of a significant discontinuity in the underlying lithologies. A zone of low resistivity (<50 Ω .m, blue colours) stretches across the entire length of the profile extending down to approximately 20 m elevation for most of the length. This is interpreted as water-saturated sands and gravels. Below this is a zone of elevated resistivity (> 100 Ω .m, yellow – red colours) extending to below 0 m elevation (river level ~14 m elevation). From the exposed fault on the riverbank (Figure 22), the material at and immediately above river level consists of weak sandstone / siltstone materials overlain by reworked volcanic sediments. Both of these layers are weakly indurated, and a resistivity similar to that expected in sandstones (Palacky, 1988) seems reasonable.

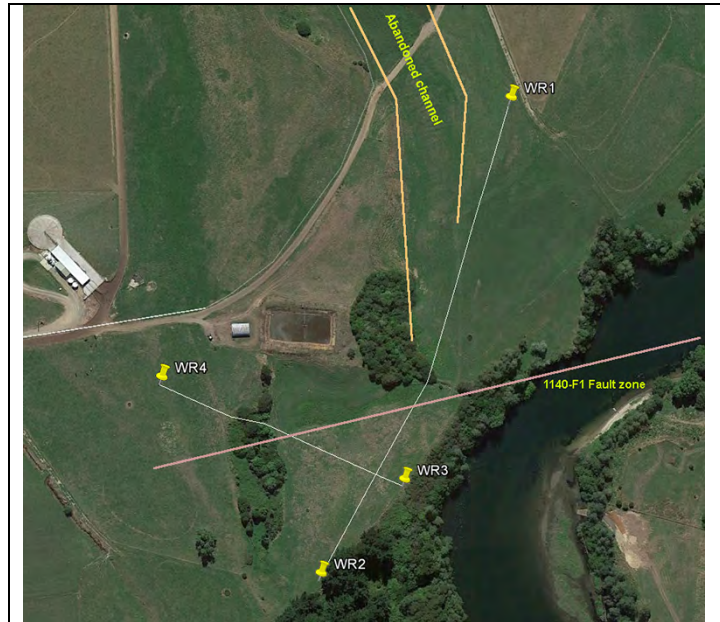


Figure 23. Resistivity survey lines at Stubbs Rd in relation to the abandoned channel and inferred location of the Te Tatu o Wairere Fault Zone.

Below this is a zone of elevated resistivity (> 100 Ω .m, yellow – red colours) extending to below 0 m elevation (river level ~14 m elevation). From the exposed fault on the riverbank (Figure 22), the material at and immediately above river level consists of weak sandstone / siltstone materials overlain by reworked volcanic sediments. Both of these layers are weakly indurated, and a resistivity similar to that expected in sandstones (Palacky, 1988) seems reasonable.

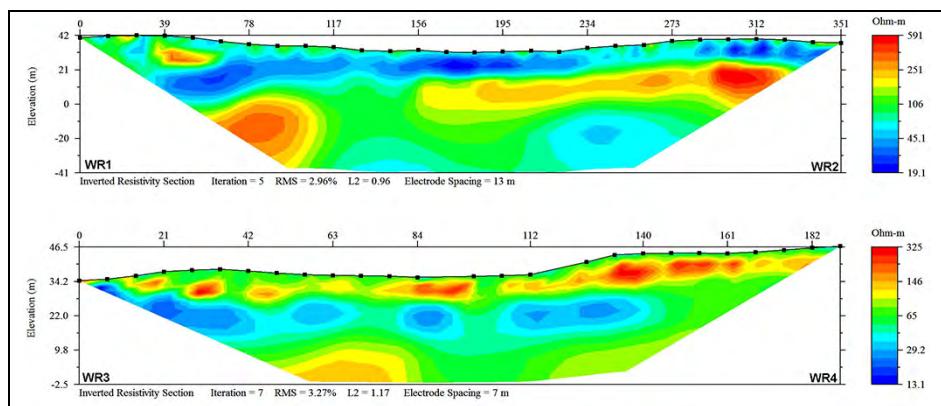


Figure 24. Resistivity results for Stubbs Rd survey lines (Figure 23): upper plot is WR1-WR2; lower plot is WR3-WR4. Note that the colour scales and the vertical scales are not the same for both surveys. Elevation is relative to mean sea level.

A break in the continuity of the high resistivity zone between approximately 117 and 150 m along the WR1-WR2 profile, suggests an offset along a steeply dipping fault zone; the overall width of this zone appears to be approximately 40 m, and the vertical offset is approximately 5 m. This amount of vertical offset is consistent with that observed across the fault zone at Kay Road. The break also occurs between 42 and 50 m along the WR3-WR4 profile, but this profile is shallower and the deeper structures are unclear. Lowered resistivity (~ 100 Ω .m,

green colour in WR1-WR2) through this zone indicates water concentration in fractures, and by comparison with Kay Road we infer a zone of fractures rather than a single fault plane. Our interpretation at this site sees the river originally flowing through the deep paleochannel, which has width and depth characteristics similar to the present river channel. Movement along the inferred fault zone (Figure 23) has caused the channel to migrate to its present course. We suggest that this may have been in stages due to the disrupted terraces located near the second bend downstream (north) from the Stubbs Rd site. Further, at some stage there was likely temporary blocking of the river, resulting in the wide embayment and terraces upstream from the site (south). We have not yet augured or drilled to see what materials comprise these terraces. Rapid entrenchment has seen the gullies and waterfall develop in response to new river course.

Assuming fault movement is the cause of the change in river channel, this occurred following entrenchment of the river as a meandering river; this dates it to post deposition of the Hinuera Formation, or within approximately the last 16,000 years.

8.2.2 Inland Port (part of Te Tatua o Wairere Fault Zone)

Geomorphic analysis and comparison with CPT data provided by Tonkin and Taylor Ltd from their investigation work on the Inland Port site for Tainui Holdings Group implies a possible fault trace displacing the Hinuera Formation near Ruakura Rd. The orientation of this trace indicates it is a likely continuation of one of a series of splays that cross the river at 1140-F2, 1153-F1, 1159-F1, 1159-F2 and 1159-F3 (Figures A6-A10), and continue along the hills on which the University is sited.

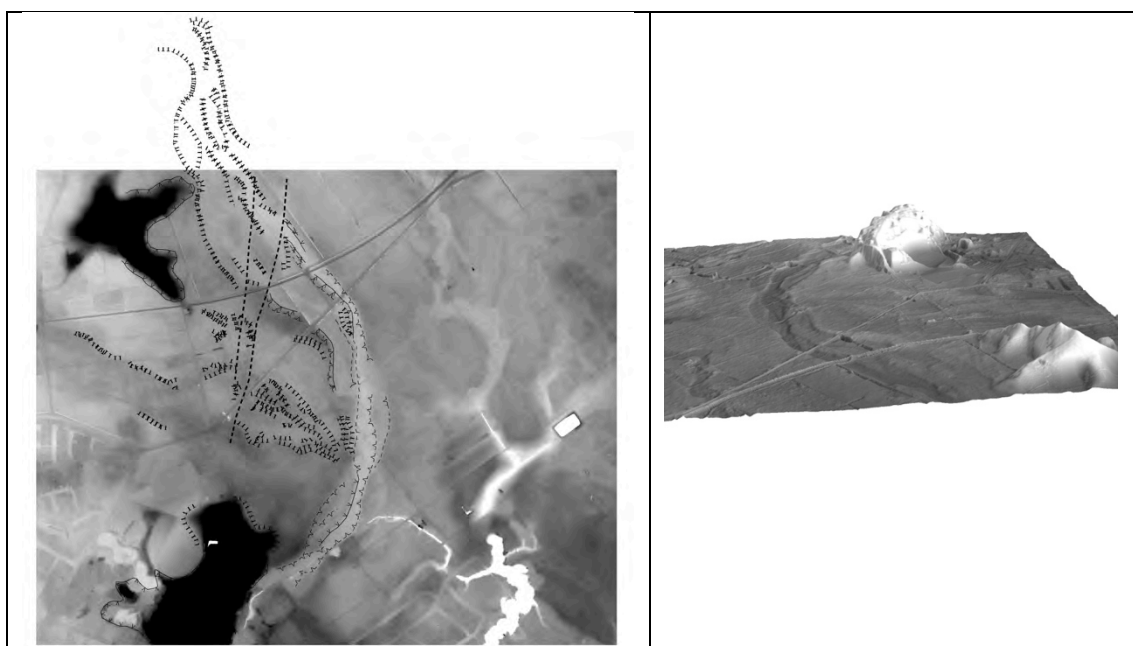


Figure 25. LiDAR and geomorphic interpretation of fault offsets of a shallow stream channel within the Hinuera Surface near the University of Waikato: (A) Plan view with geomorphic interpretation (University located in lower left corner); (B) vertically exaggerated DTM of the LiDAR data looking southwards (Curving embankment is the Hamilton-Tauranga railway line).

Geological mapping along the riverbank between Hamilton Gardens and Hammond Park have provided some evidence for these faults displacing units on land. These data are still being analysed and interpreted as part of an MSc thesis project.

8.2.2.1 Resistivity

Due to the availability of CPT, drill hole and test pit data (Figure 26) for comparison with resistivity data, the Inland Port site was used to test a 3D upgrade to the resistivity survey equipment. A small area of the site was selected primarily based on ease of access and avoiding interference with activities on the Inland Port site. However, the surveyed area did intersect the faulting inferred from the LiDAR data (Figure 25 left). The survey used the

dipole-dipole gradient approach with an electrode spacing of 11 m to provide a maximum survey depth of ~45 m for the 3D analysis.

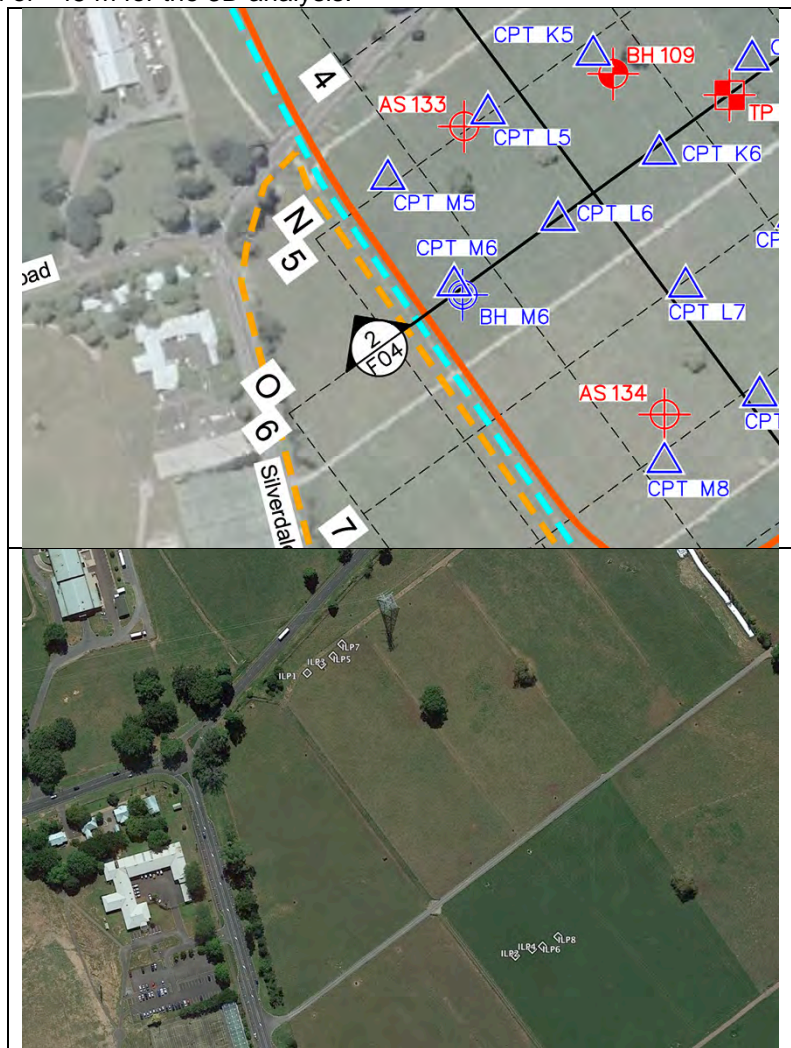


Figure 26. Section of the Inland Port site next to the University of Waikato showing (upper) the location of CPT, borehole (BH) and test pit (TP) data obtained by Tonkin and Taylor Ltd, and (lower) the endpoints of resistivity survey lines collected by the University. Also marked on the upper images are cross-sections interpreted by Tonkin and Taylor Ltd (solid black lines).

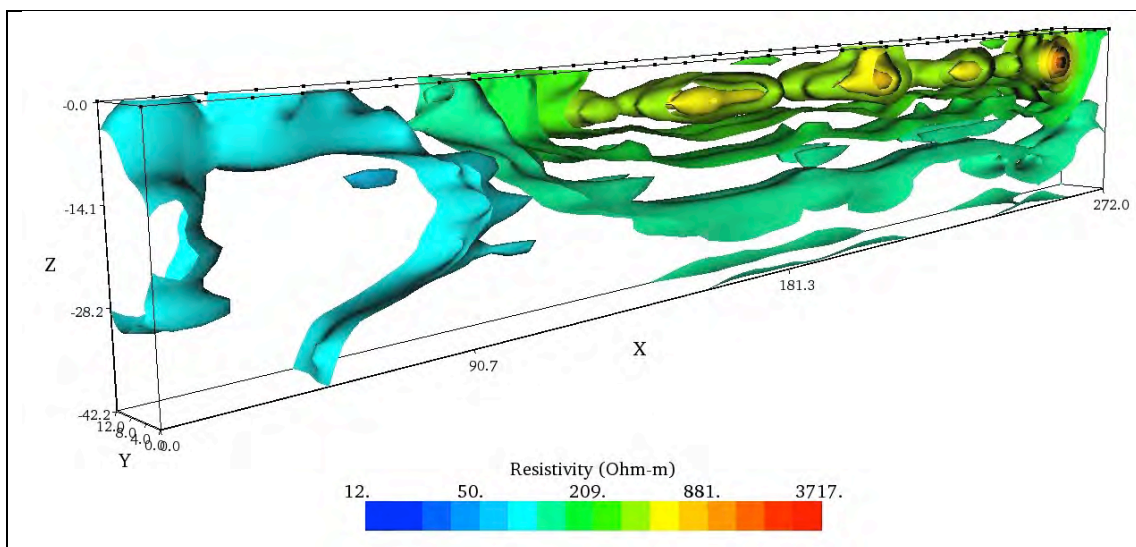


Figure 27. Three-dimensional visualisation of the resistivity survey data for the Inland Port site. The elevation is measured relative to the ground surface.

The resistivity data indicate the presence of a dipping structural break at ~90 m (Figure 27) from the northern boundary of the surveyed area (Figure 26). The Tonkin and Taylor Ltd interpretation for section 3, which is closest to the resistivity survey, indicates a sequence of sands and gravels north of the break consistent with the low resistivity. South of the break, the Tonkin and Taylor Ltd data indicate the presence of multiple silt/clay and organic rich layers within sands and gravels, producing highly variable resistivity.

We infer the presence of a southwards dipping fault. Provided that the work can be scheduled around construction activities, we consider that this will be a good location for trenching.

8.3 Horotiu Fault Zone (Osborne Road)

Similar to Stubbs Rd, a site at the northern margin of Hamilton City also shows considerable offset in the river (1326-F1 and 1326-F2, Figures A18 and A19). This aligns with a subtle surface feature consisting of a monoclinical rise in the ground surface trending towards the north-northeast from the river and running roughly parallel to Osborne Road. The vertical offset across this is 2 – 3 m over a width of 50 m (Figure 28A). While this is subtle, it is a persistent linear feature that appears on the LiDAR, and is not clearly related to stream / gully formation within the area. Persaud *et al* (2016) report that sections of the Kerepehi Fault occur as monoclinical folds. The importance of this feature comes from the fact that it displaces the Late Pleistocene Hinuera Formation. It may also be significant that a cluster of peat lakes along the alignment of the surface feature all contain disrupted tephra layers that are thought to represent seismites.

8.5.1 Geomorphology

Several features existed on the seismic traces near the inferred fault zone at Horotiu. Of these, one, the trace near Osborne Road (Figure A18) is most strongly suggestive of faulting. This location is 3.2 km south of our original estimated position near the Horotiu Bridge (1340-F1, Figure A20), and most likely reflects the fact that there is splintering of the near surface fault(s) in this area.

Detailed analysis of the geomorphology in this area reveals a terrace running approximately southwest – northeast to the north of the river. This terrace has a vertical offset of 2 – 3 m (Figure 28A), and runs approximately normal to the “fabric” of the Hinuera Surface. We infer that this may represent a relatively recent (< 16,000 years) offset along a fault as it disrupts the Hinuera Surface.

There is also evidence for an abandoned channel on the western bank of the river between Hutchinson Rd and Horotiu Bridge Rd. However, due to sand extraction and construction of the bridge approaches for the Waikato Expressway, detailed mapping of the original geomorphology has not been possible to date.

8.5.2 Resistivity

A 3-dimensional survey was undertaken across the monoclinical feature parallel to Osborne Rd, with 8 lines of approximately 70 m length running normal to the strike of the lineation. With a closer electrode spacing, this survey was intended to give high resolution data to a

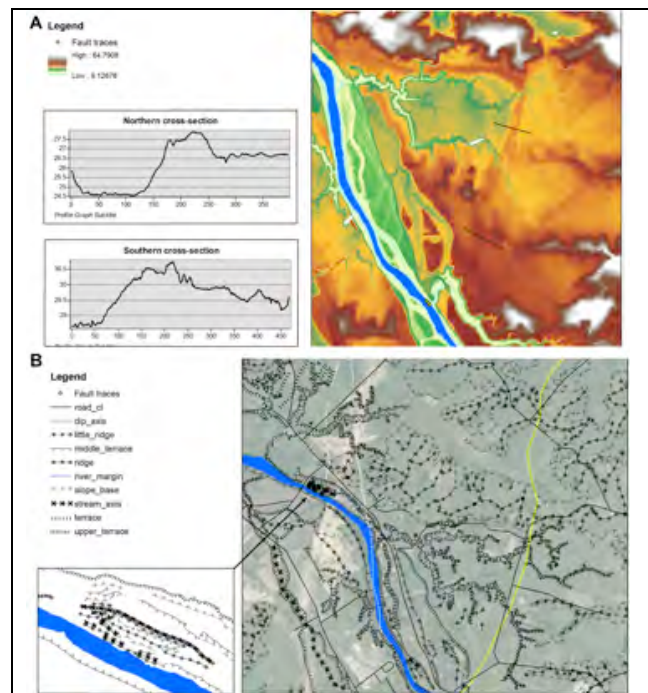


Figure 28: Geomorphological analysis of Osborne Road site. (A) LIDAR showing lineation with profiles showing vertical offset of approximately 2 m as indicated by the cross-sections, and (B) fault location inferred from geomorphology; inset shows location of a possible lateral spread feature by the Horotiu bridges.

relatively shallow depth of approximately 15 m. Figure 29A gives a representative 2D inverted profile (line 1), while Figure 29B gives the 3D reconstruction of the site.

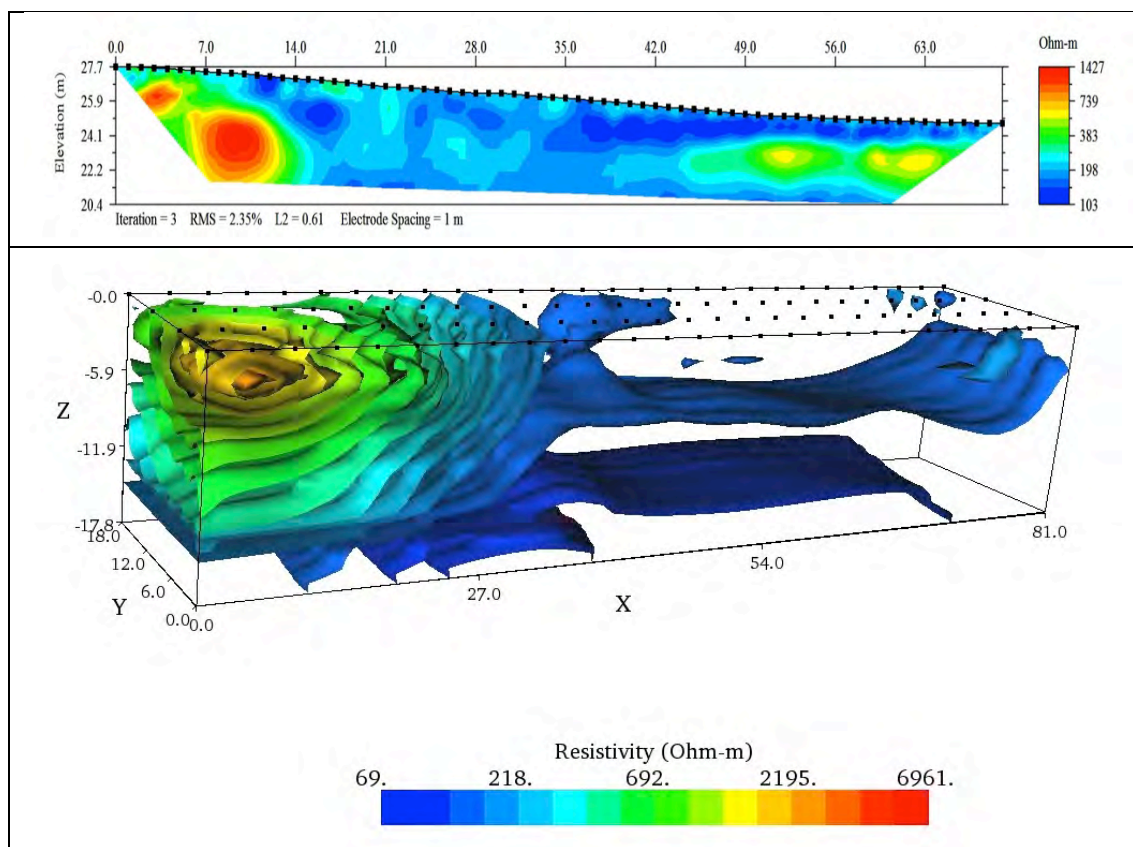


Figure 29. Resistivity survey results for Osborne Rd: (A upper panel) an example of one of the resistivity profiles used for the 3D analysis (Elevation relative to mean sea level); and (B lower panel) 3D analysis of 8 profiles (Elevation relative to highest survey point). Note that the 3D analysis extends to a greater depth than the 2D resistivity survey

There looks to be a fault offsetting the Hinuera Formation at the position of the observed lineation in the LiDAR data. However, compared to the previous resistivity survey results discussed above, the 3D visualisation (Figure 29B) suggests the presence of a reverse fault. Persaud *et al* (2016) noted a similar feature in the Madill Trench across the Te Poi segment of the Kerepehi Fault (Caption Figure S3 of their Supplementary Information). This is illustrated in Figure 12D above, and was interpreted as toppling of the fault planes towards the downthrown side.

A series of auger holes were undertaken to profile normal to the lineation for comparison with the resistivity survey. These confirmed the resistivity results, with an area of oxidised silty clays and sands on the upthrown side (0-10 m on resistivity profile), a complex zone along the slope (14-40 m on profile), and a zone of flat-lying sediments (predominantly silty clays) on the lower elevation surface (42-60 m on profile).

We consider that a fault is present at this site, and this would be a suitable site for trenching. As construction of the Hamilton Section of the Waikato Expressway continues, earthworks are scheduled for a crossing of Osborne Rd. However, this may not involve excavation to a depth that would be useful for examining the fault zone.

9 . Volcanoes

Kear and Schofield (1965) identified exposures of volcanic rocks near Koromatua on their geological map (Figure 30A), but it is unclear what evidence this was based on. These are not mapped on the QMap sheet due to the lack of any verified surface exposures of primary volcanic rock (Briggs, *pers. comm.*). However, the geomorphology interpreted from the LiDAR and from site examinations indicate that the two volcanic craters mapped by Kear and Schofield (1965) do exist. The LiDAR data also indicate the presence of similar features, which are not easily visible from the roadside. The inferred volcanic craters are aligned in a

zone parallel to the Kukutaruhe Fault Zone (Figure 30B), and the alignment of geothermal activity previously recognised within the Hamilton Basin (Schofield, 1972). Schofield (1972) noted that borehole temperatures increased from Templeview towards the Waikato River, with the highest temperatures associated with thermal baths (now closed) near the intersection of Aberfoyle and Rifle Range Roads in Frankton.

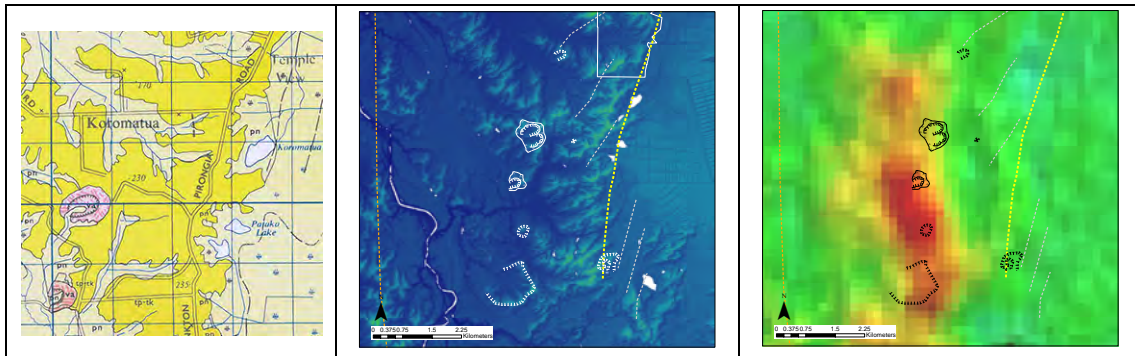


Figure 30. Volcanic features at Koromatua: (A left) distribution of volcanic rocks depicted on the N65 sheet; (B centre) locations of craters inferred from geomorphology, with the location of the Kukutaruhe Fault Zone determined from LiDAR marked by yellow dashed line; and (C right) location of the magnetic anomaly at Koromatua with the geomorphology mapping interpretation superimposed.

As well, although the georeferencing and resolution is poor, there appears to be a magnetic anomaly aligned with the volcanic features at Koromatua. At present we have no data to constrain the age of these volcanic events, although Kear and Schofield (1965) suggest that they are part of the Pirongia Volcanics within the Alexandra Volcanics, with a Late Pliocene-Early Pleistocene age. The volcanic features also lie at the junction between the inferred Waipa Fault and the Kukutaruhe Fault Zone.

10. Our present interpretation

Figure 31 summarises the pattern of faults identified by all of the approaches discussed above. So far the identified faults are all clustered in the western half of the Hamilton Basin. This is the area that has the largest amount of subsurface data available, as well as geomorphic features that can be associated with faulting.

The eastern sector is relatively flat with few hills, and is mostly covered by peat (Komakorau Swamp) that tends to mask the underlying geomorphology. One feature that is evident in the LiDAR data underlying Figure 31 is that the drainage network (Komakorau Stream) in the northeastern sector runs parallel to the Waikato River until it eventually joins the Mangawara Stream, which flows westward along the foot of the Taupiri Block, close to Taupiri. There are very limited data on the thickness of the peat deposit within the Komakorau peat swamp, and the depth to basement beneath the peat.

The gravity (Figure 5A) and deep seismic data suggest that the Hamilton Basin is divided into two separate sub-basins, with the larger and deeper western basin lying between Hamilton

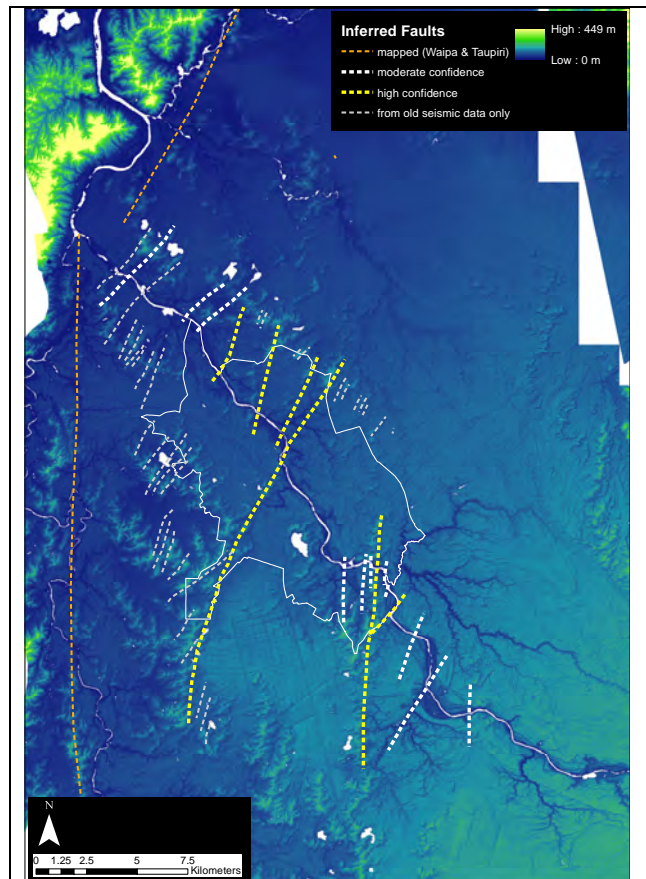


Figure 31. Inferred faults with the Hamilton Basin colour-coded with the present level of confidence that we have in the indicated fault being a real feature.

and Ngaruawhia, and a smaller shallower eastern basin between Hamilton and Gordonton. The faults identified within the western sub-basin appear to terminate against a northwest-southeast trending “ridge”. However, the presence of geothermal fluids at Orini in the northeast of the Hamilton Basin suggests that faults are likely to be present, but these may not connect to those already identified.

Due to the lack of data for the eastern half of the Hamilton Basin, we have focussed on the western sector. For this sector, the gravity anomaly (Figure 5A) was taken as a proxy for the depth to basin, which was calibrated by the Te Rapa-1 exploration well. This was used to constrain the interpretation of the older oil and gas exploration seismic data (Figure 10). We interpret the deeper seismic data as showing a pattern of major southwards dipping normal listric faults (Figure 32), which form a series of half grabens (Hamilton Hills). Numerous smaller synthetic and antithetic faults occur between the main fault zones, creating a complex pattern of small horsts and grabens similar to the Basin and Range Province in the USA (Figure 33). This proposed structure differs significantly to the sub-horizontal layer-cake stratigraphy assumed for previously published cross-sections (Figures 3A, 3B and 4).

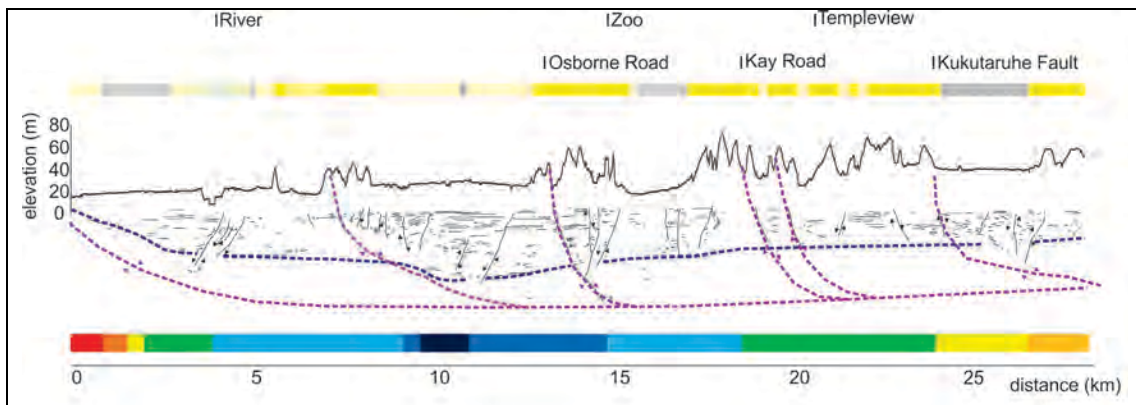


Figure 32. Interpreted seismic section of Line PR569-2 (Liles, 1971) as shown in Figure 10 with inferred listric faults included in magenta. The depth to which these extend in the basement is unknown, so the depth shown here is purely schematic.

Based on the gravity data and the seismic line interpretation, we consider that the listric faults extend into a detachment surface within the basement greywacke, with steep dips to the north and flattening towards the south. This pattern of faulting results in the “Hamilton Hills” which consist of Pliocene–Pleistocene Walton Subgroup materials overlain by rhyolitic tephra sequences. These hills tend to have steeper slopes on the southern sides and gentler slopes on the northern side (Figure 33). The tilted blocks of Walton Subgroup sediments form a series of half-grabens that are partially infilled with late Pleistocene Hinuera Formation sediments and peat bogs. Antithetic and reverse faults appear to cluster at the northern end of the half-grabens, representing fracturing which allows accommodation space (rollovers) against the steeply dipping section of the fault system. The fracturing introduces additional complexity in the geomorphology.

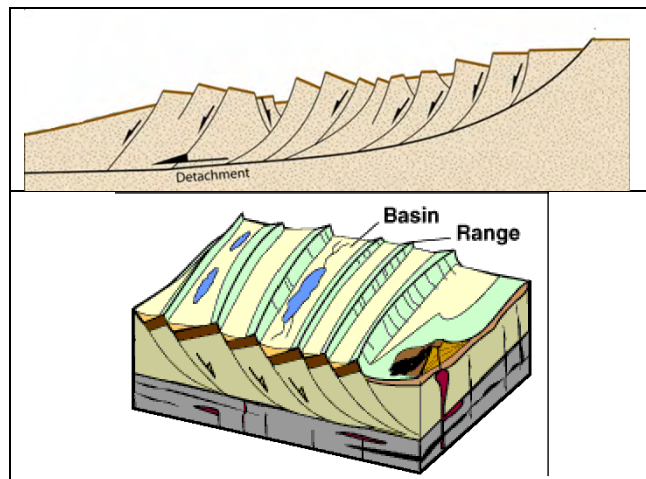


Figure 33. Schematic diagrams of listric faulting with synthetic and antithetic faults producing a sequence of small horsts and grabens (After Eaton, 1979; and <http://www.sagaingfault.info/>).

One remaining problem is what happens at the southern end of the Hamilton Basin. It is clear that the pattern of faulting associated with the Waipa Fault is different in this region (viz. Kirk, 1991). Basement rocks are exposed along the southeastern boundary of the Hamilton Basin between Otorohanga, Karapiro and Morrinsville, which may indicate that the detachment surface daylight somewhere in the south.

11. Risk assessment

Assuming that the methodology used by Persaud et al (2016) for the Kerepehi Fault segments is also applicable to the faults within the Hamilton Basin, it is possible to estimate the maximum credible earthquake (MCE) associated with the fault segments in Figure 31. Figure 34 compares the MCE for a ~25 km fault rupture within the Hamilton Basin with the predicted values for Hamilton City based on different rupture scenarios for the Kerepehi Fault. The MCE magnitude corresponds to Mw 6.6, with a maximum MM Intensity of 9-10. These data suggest that the shaking intensity within Hamilton City will be significantly greater due to a local earthquake than predicted for the Kerepehi Fault. Research is now focussing on obtaining data to determine the frequency of rupture within the Hamilton Basin. This includes a student project undertaking a review of historical records and oral histories of local iwi, which has so far identified several damaging events during the 1800s.

We have been in discussion with other researchers at the University of Auckland and GNS about the significance of the distribution of faults depicted in Figure 31 in terms of the tectonic regime. We are now aware that there are some GPS sites within the basin that could be used to assess the relative slip rates, which would be useful to examine.

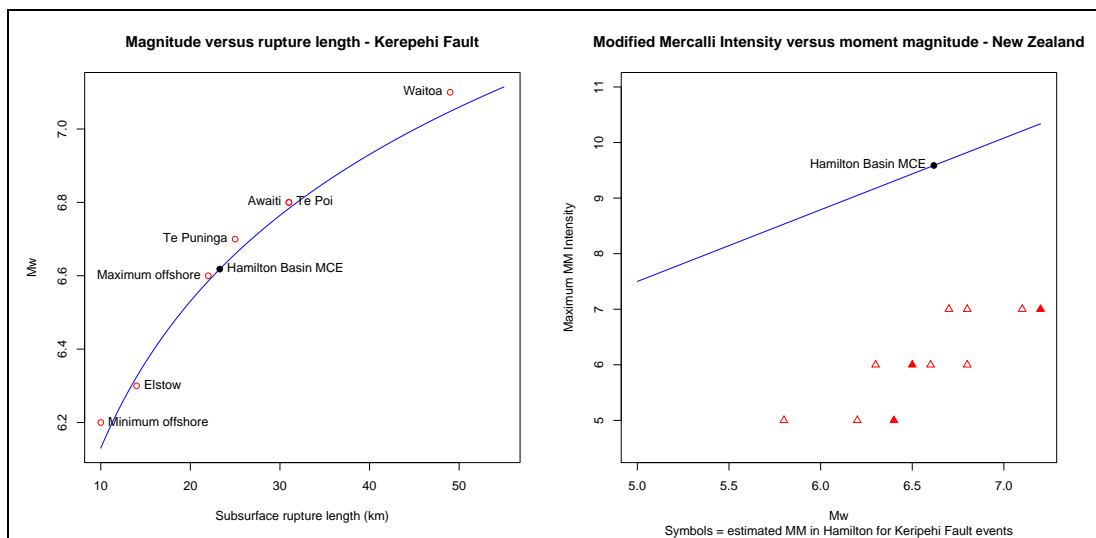


Figure 34. Calculated maximum magnitude (left) and Modified Mercalli Intensity (right) for the largest fault rupture length in Figure 31, and those predicted for Hamilton City for rupture of the Kerepehi Fault segments by Persaud *et al* (2016).

11. References

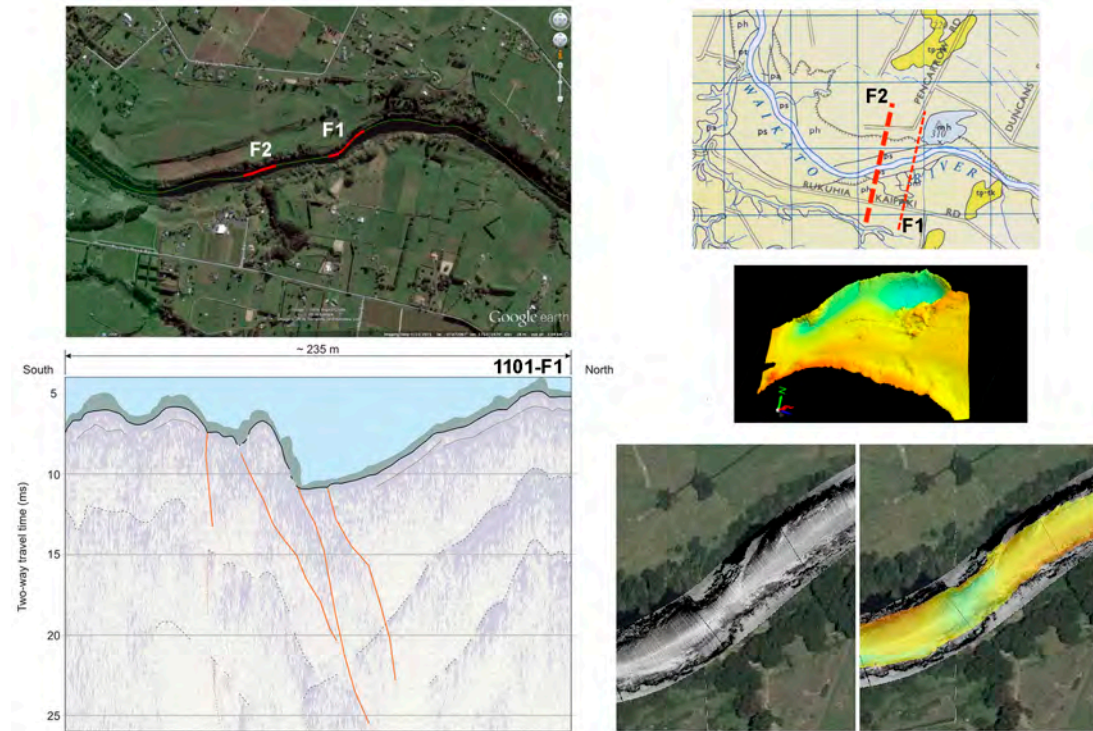
- Eaton, G.P., 1979. Regional geophysics, Cenozoic tectonics, and geologic resources of the Basin and Range Province and adjoining regions.
- Edbrooke, S.W. (compiler), 2005. Geology of the Waikato Area. Institute of Geological and Nuclear Sciences 1:250,000 map 4. Institute of Geological and Nuclear Sciences, Lower Hutt. 1 sheet + 68 p.
- Edbrooke, S., Ricketts, B, and Leonard, G., 2009a. Opportunities for underground geological storage of CO₂ in New Zealand – Report CCS-08/2 – The onshore Waikato Region. *GNS Science Report 2009/54*, November 2009, 72 p.
- Edbrooke, S., Clemens, A., Matheson, T., Pope, J., Rumsey, B., Weeks, C., St George, J., Seifert, S., Winans, R., Bain, E. and Calo, J. 2009b. Opportunities for underground geological storage of CO₂ in New Zealand - Report CCS-08/3 - The Waikato and King Country coal resource. *GNS Science Report 2009/55*. November 2009, 121 p.
- FrOG Tech, 2011. Waikato structural GIS and SEEBASE™ Project: Phase 1 November 2010, FrOG Tech Project Code CWE701 and Phase 2 November 2011, FrOG Tech Project Code CWE703. Ministry of Economic Development New Zealand Unpublished Petroleum Report PR 4432.
- Heron, D.W. (custodian), 2014. Geological Map of New Zealand 1:250 000. GNS Science Geological Map 1. Lower Hutt, New Zealand.

- Houghton, B.F., and Cuthbertson, A.S., 1989. *Sheet T14 BD – Kaimai*. Geological map of New Zealand 1:50 000. Map (1 sheet) and notes. Wellington, New Zealand. Department of Scientific and Industrial Research.
- Hume, T.M., 1972. *The petrology of the Hinuera Formation*. MSc Thesis, Department of Earth Sciences, University of Waikato.
- Hume, T.M., Sherwood, A.M., and Nelson, C.S., 1975. Alluvial sedimentology of the Upper Pleistocene Hinuera formation, Hamilton Basin, New Zealand. *Journal of the Royal Society of New Zealand* 5(4): 421-462.
- Hunt, T.M., 1978. Stokes magnetic anomaly system. *New Zealand journal of geology and geophysics* 21(5): 595-606.
- Kear, D., 1960. Sheet 4 – Hamilton. Geological Map of New Zealand 1:250,000. Department of Scientific and Industrial Research, Wellington, New Zealand.
- Kear, D., and Schofield, J.C., 1965. N65 – Hamilton. Geological Map of New Zealand 1:63,360. Department of Scientific and Industrial Research, Wellington, New Zealand.
- Kear, D., and Schofield, J.C., 1966. N56 – Ngaruawahia. Geological Map of New Zealand 1:63,360. Department of Scientific and Industrial Research, Wellington, New Zealand.
- Kirk, P.A., 1991. Waipa Fault and the tectonic rotation of the Hakarimata-Taupiri Block. *New Zealand Geological Survey Record* 43: 81-84.
- Liles, V.E., 1971. Seismic survey, Waikato Basin 1970-71. Ministry of Economic Development New Zealand Unpublished Petroleum Report PR 569.
- Lowe, D.J., 1981. *Late Quaternary air-fall deposits, Hamilton Basin, New Zealand*. MSc Thesis, Department of Earth Sciences, University of Waikato. 391 p.
- Lowe, D.J., Tipett, J. M., Kamp, P.J.J., Liddell, I.J., Briggs, R.M., Horrocks, J.L., 2001. Ages on weathered Plio-Pleistocene tephra sequences, western North Island. New Zealand. *In: Juvigné, E. T., Raynal, J. P. (Eds), Tephros: Chronology, Archaeology, CDERAD éditeur, Goudet. Les Dossiers de l'Archéo-Logis* 1: 45-60.
- Manville, V., and Wilson, C.J.N., 2004). The 26.5 ka Oruanui eruption, New Zealand: A review of the roles of volcanism and climate in the post-eruptive sedimentary response, *New Zealand journal of geology and geophysics*, 47(3): 525-547
- McLintock, A.H. (editor), 1966. South Auckland Land District. *In An Encyclopedia of New Zealand*. <http://www.TeAra.govt.nz/en/1966/geology-land-districts-of-new-zealand/page-2>
- Meyers, J., 2009. Report on the titanomagnetite sands for the period ending March 2009. Ministry of Economic Development New Zealand Unpublished Mineral Report MR 4482.
- Morisawa, M., 1968. Classification of Rivers. *In Fairbridge, R.W. (ed.), The Encyclopedia of Geomorphology*, New York: Reinhold Book Corporation, pp. 956–957
- Palacky, G.J., 1988. Resistivity Characteristics of Geologic Targets. *In Nabighian, M.N., and Corbett, J.D. (eds.), Electromagnetic Methods in Applied Geophysics: Volume 1, Theory*. Society of Exploration Geophysicists. 52-129.
- Persaud, M., Villamor, P., Berryman, K.R., Ries, W., Cousins, J., Litchfield, N., and Alloway, B.V. 2016. The Kerepehi Fault, Hauraki Rift, North Island, New Zealand: active fault characterisation and hazard. *New Zealand journal of geology and geophysics* 59:117-135.
- Schofield, J.C., 1965. The Hinuera Formation and associated Quaternary events. *New Zealand journal of geology and geophysics* 8(5): 772-791.
- Schofield, J.C., 1972. Ground Water of Hamilton Lowland. *New Zealand Geological Survey Bulletin* 89 , 71 pp.
- Sherwood, A.M., 1972. *Sedimentary structures, texture, and paleoenvironment of the Hinuera Formation*. MSc Thesis, Department of Earth Sciences, University of Waikato.
- Wood, A.P., 2006. Morphodynamic channel and stability of the Waikato River: Karapiro to Ngaruawahia Reach. Unpublished MSc thesis, University of Waikato, Hamilton. 393 p + CD-ROM

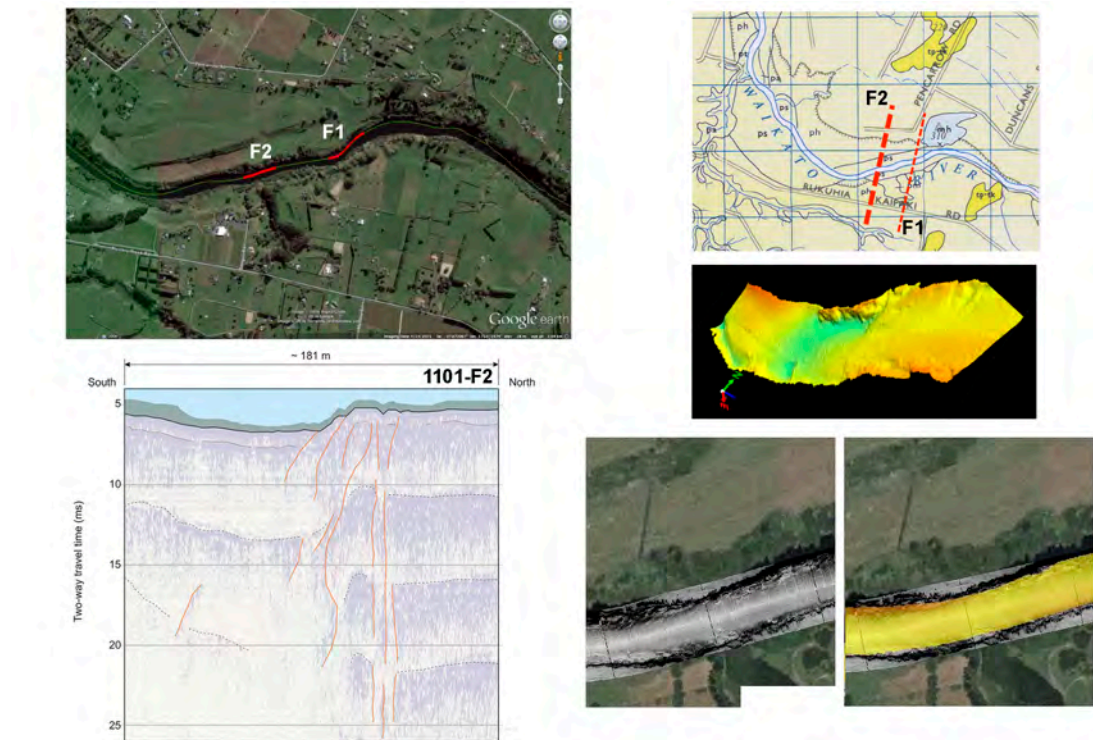
12. Acknowledgements

We thank the EQC for funding support via Biennial Grant 16/717. Waikato Regional Council provided LIDAR data and funding support for 3 associated MSc projects, and the University of Waikato provided Summer Scholarship support for 2 students. We acknowledge the contributions of Ben Campbell, Riley Cochrane, Mike Cummins, Aleesha McKay, Tom Robertson, and Francesca Spinardi for fieldwork and data analysis.

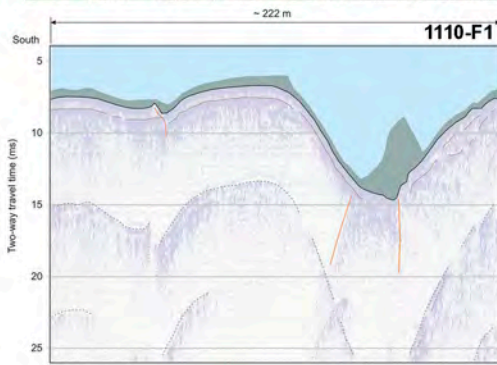
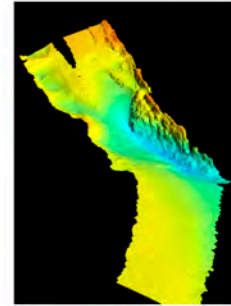
13. Appendix A



A1: 1101_F1 Greywacke Hill
 Zone -37.8705061 175.3745269 to -37.8708992 175.3740692, 59 m wide.



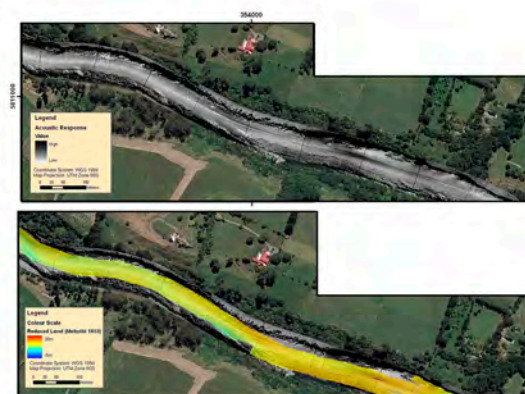
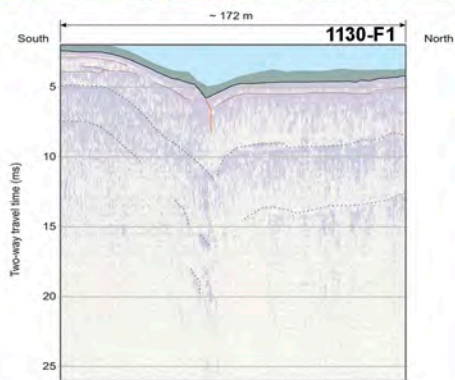
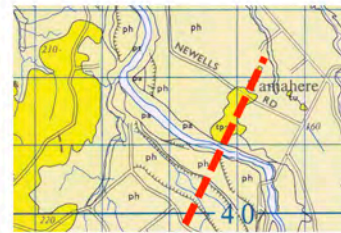
A2: 1101_F2 Mystery Creek
 Zone -37.8720244 175.3688811 to -37.8721542 175.3684692, 39 m wide.



A3: 1110_F1 Lochiel

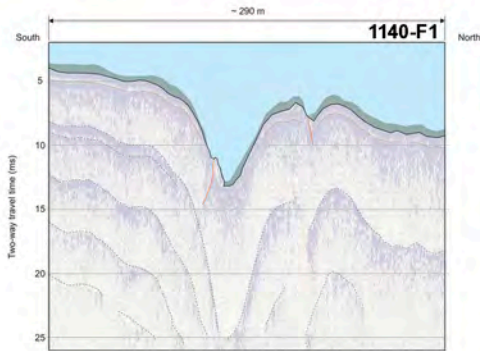
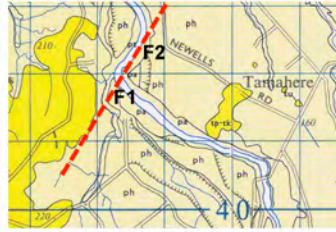
Discontinuity at -37.8627928 175.3506622

Zone -37.8620453 175.3500211 to -37.8619117 175.3498228, 23 m wide



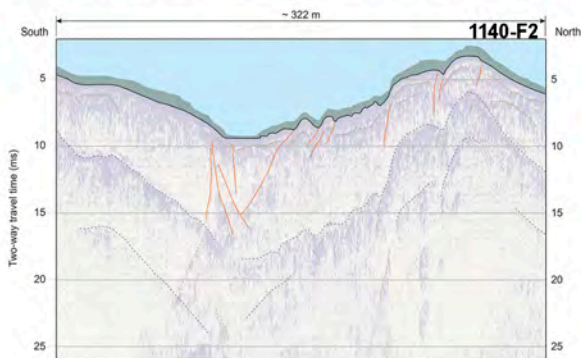
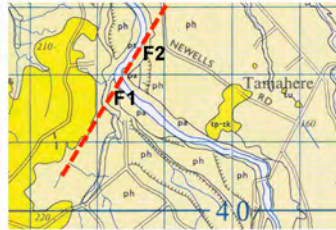
A4: 1130_F1 The Narrows

Discontinuity at -37.8377075 175.3425292



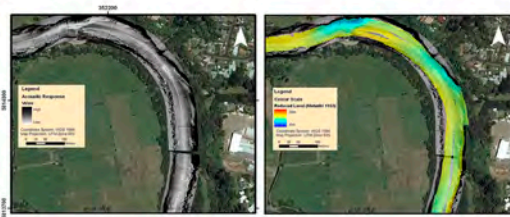
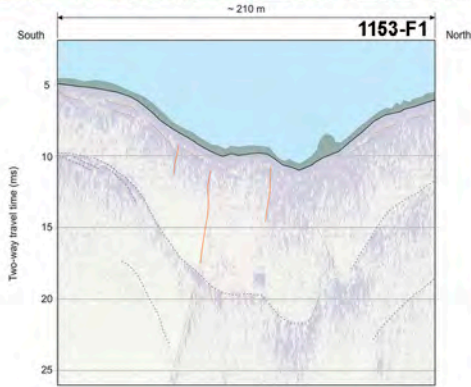
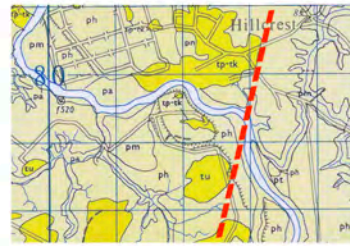
A5: 1140_F1 Stubbs Road

Discontinuities at -37.8282356 175.3258969 and -37.8277739 175.3260497



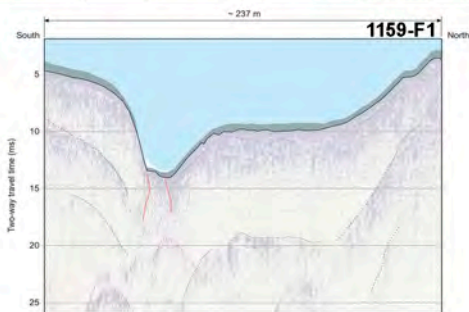
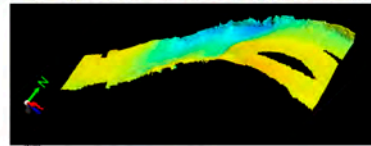
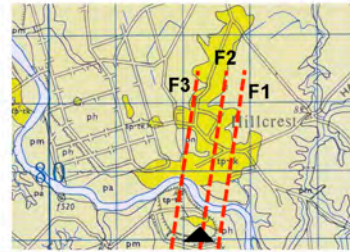
A6: 1140_F2 Riverglade Drive

Zone -37.8248061 175.3298950 to -37.8233528 175.3305358, 171 m wide



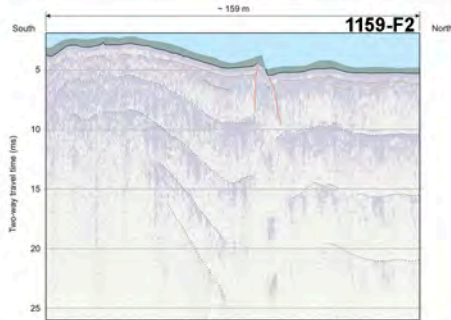
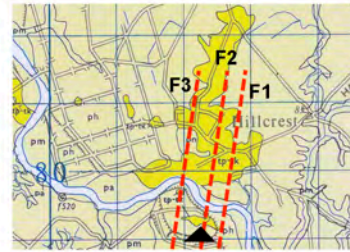
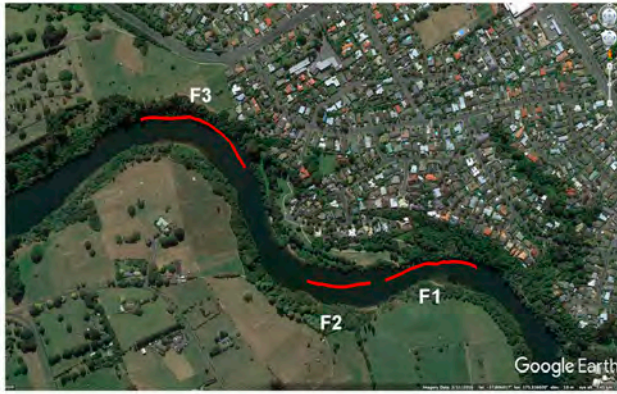
A7: 1153_F1 Silvia Crescent

Zone -37.8088569 175.3229978 to -37.8083342 175.3225706, 69 m wide



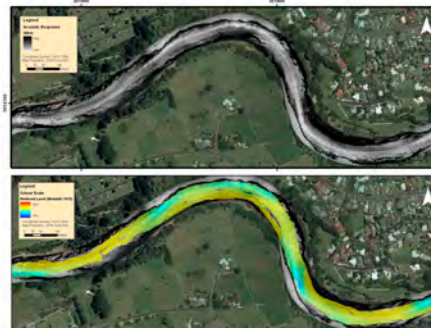
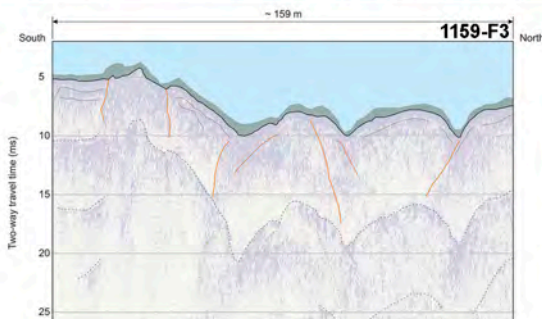
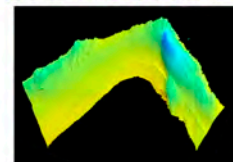
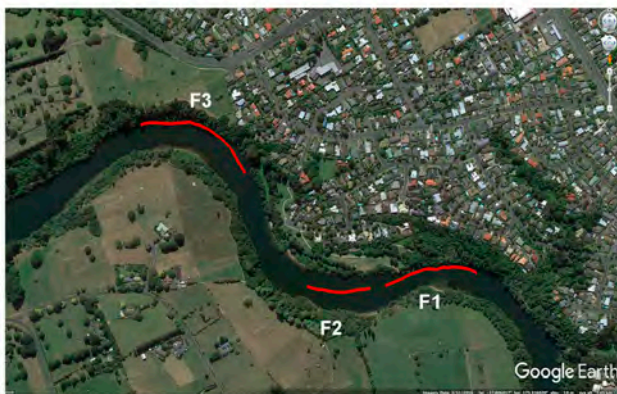
A8: 1159_F1 Hammond Park

Zone -37.8074644 175.3204956 to -37.8074569 175.3203428, 13 m wide



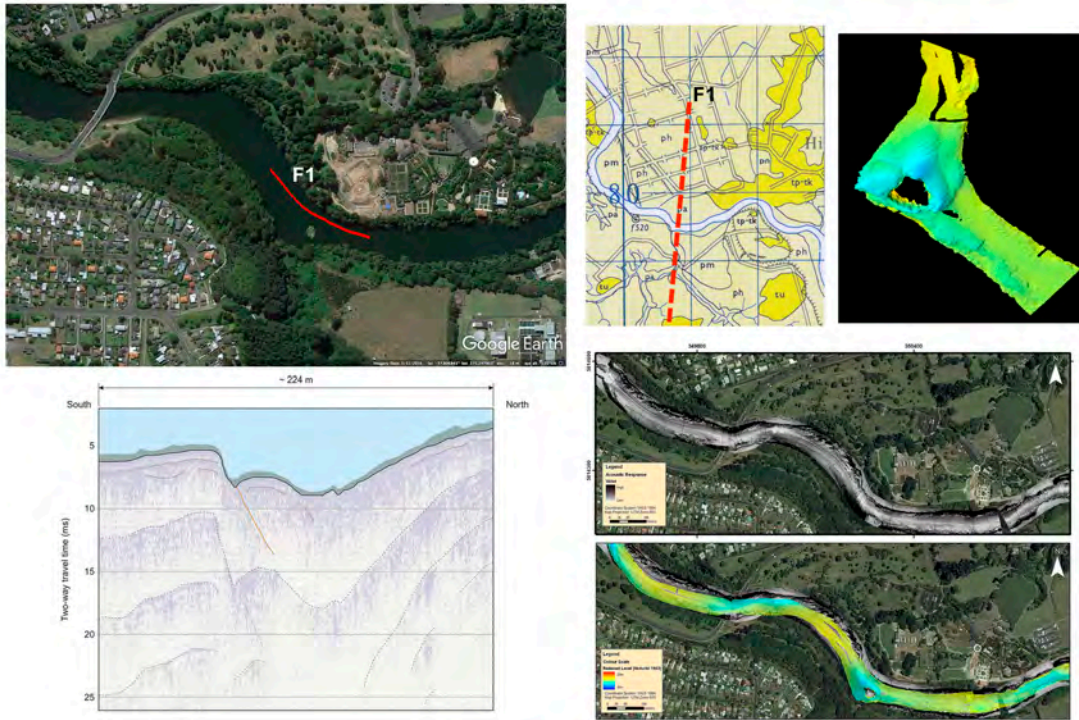
A9: 1159_F2 Hammond Park

Zone -37.8079908 175.3172300 to -37.8079719 175.3170928, 12 m wide

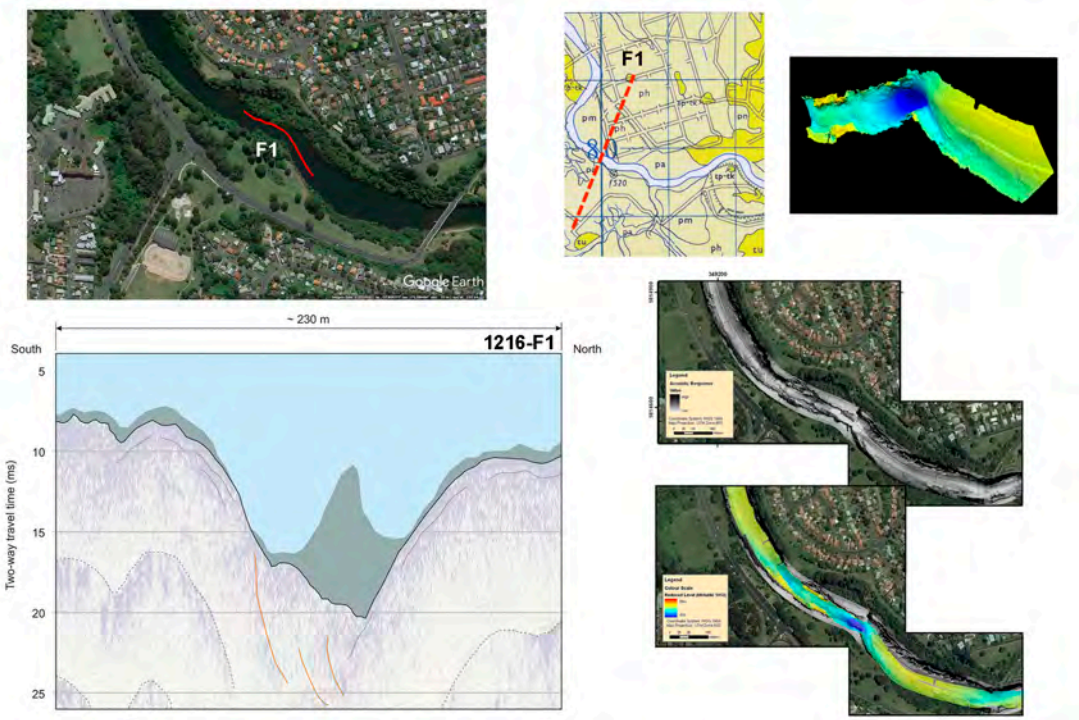


A10: 1159_F3 Wairere Ring Road

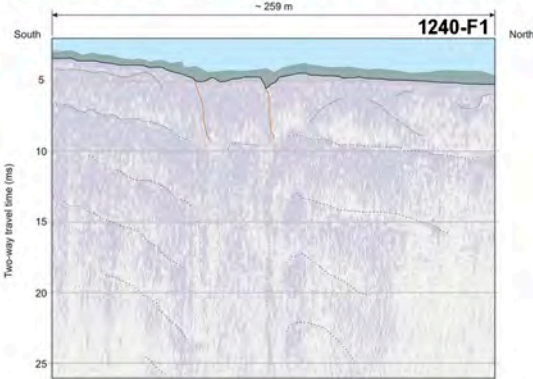
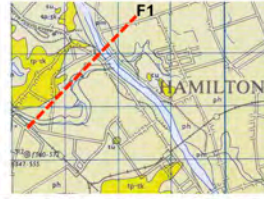
Zone -37.8052747 175.3146056 to -37.8043403 175.3121642, 239 m wide



A11: 1210_F1 Hamilton Gardens
 Zone -37.8074225 175.2995603 to -37.8072775 175.2992094, 35 m wide

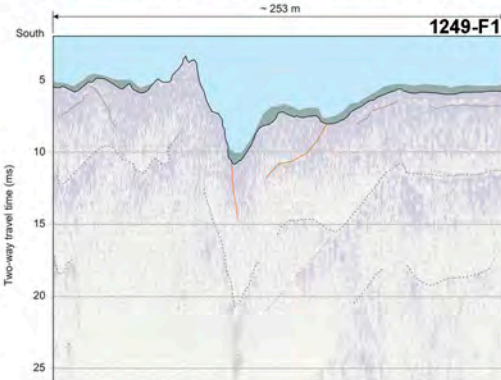
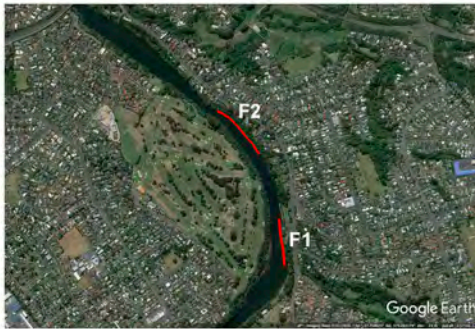


A12: 1216_F1 Graham Island
 Zone -37.8039969 175.2910764 to -37.8037108 175.2906950, 46 m wide



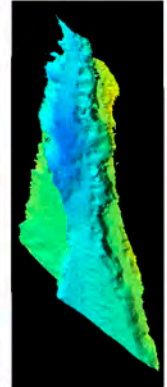
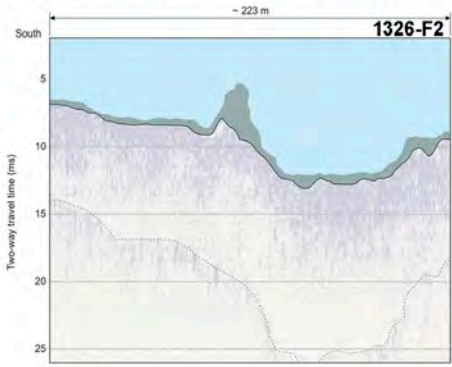
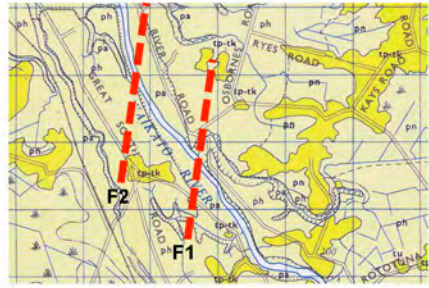
A13: 1240_F1 Fairfield Bridge

Zone -37.7718694 175.2702178 to -37.7715681 175.2699583, 41 m wide

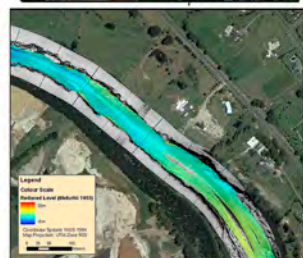
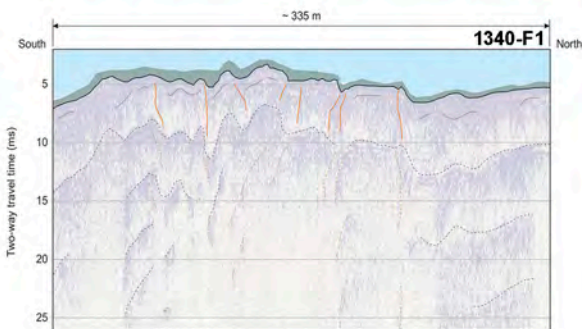
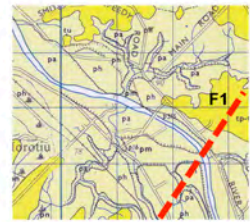


A14: 1249_F1 Swarbrick Landing

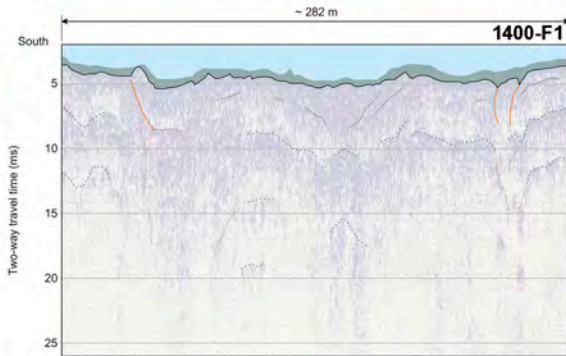
Discontinuities at -37.7549781 175.2664947 and -37.7543067 175.2663878



A19: 1326_F2 Pukete Boat Ramp
Discontinuity at -37.7182731 175.2221525

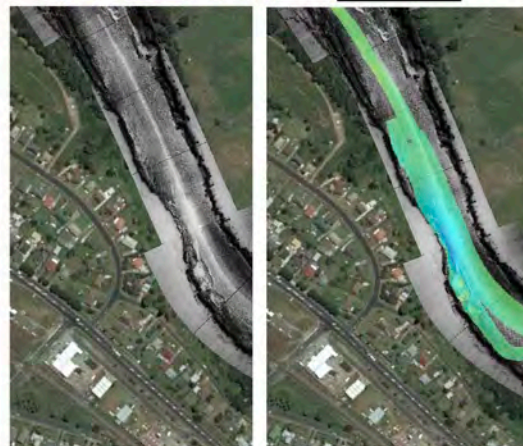
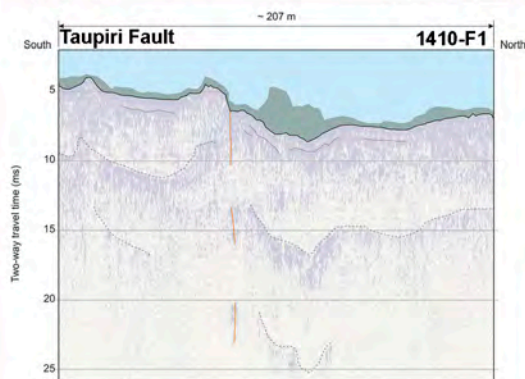
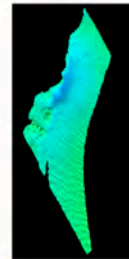


A20: 1340_F1 Horotiu Bridge
Zone -37.7033919 175.2163083 to -37.7018356 175.2155914, 184 m wide



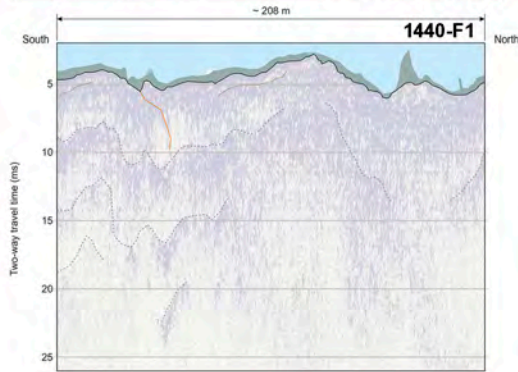
A21: 1400_F1 Amani Lane

Zone -37.6804428 175.1762083 to -37.6801414 175.1737211, 222 m wide

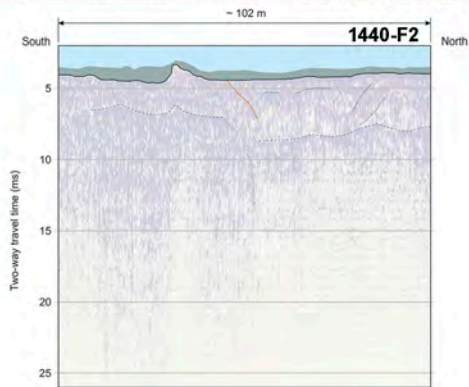


A22: 1410_F1 Waikato Esplanade South

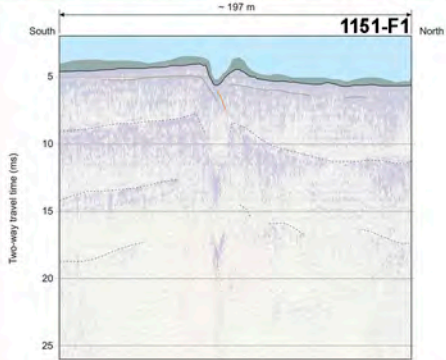
Discontinuity at -37.677704 175.164994



A23: 1440_F1 Hopuhopu
 Discontinuity at -37.6453781 175.1506194



A24: 1440_F2 Hopuhopu
 Zone -37.6413000 175.1506042 to -37.6406819 175.1508331, 72 m wide



A25: 1511_F1 Taupiri
 Discontinuity at -37.6206206 175.1858825